Characterization of Iron-Imido Species Relevant for *N*-Group Transfer Chemistry

Diana A. Iovan and Theodore A. Betley*

Department of Chemistry and Chemical Biology

Harvard University

12 Oxford Street, Cambridge, MA 02138

Page

General Considerations. All manipulations of metal complexes were carried out in the absence of water and dioxygen using standard Schlenk techniques, or in an MBraun inert atmosphere drybox under a dinitrogen atmosphere. Ligand and ligand precursors were synthesized as previously reported.[1] All glassware was oven dried for a minimum of 1 hour and cooled in an evacuated antechamber prior to use in the drybox. Benzene, diethyl ether, dichloromethane, *n*-hexane, pentane, toluene, fluorobenzene and tetrahydrofuran were dried over 4 Å molecular sieves (Strem) prior to use. Chloroform-*d* was purchased from Cambridge Isotope Labs and used as received. Benzene-d_6 was purchased from Cambridge Isotope Labs and was degasses and stored over 4 Å molecular sieves prior to use. 3,5-bis(trifluoromethyl)aniline, 2,6-diisopropylaniline, sodium azide, sodium nitrite, *tert*-butyl nitrite, trimethylsilyl azide, 1,4-cyclohexadiene, styrene, cyclohexene, 1,5-cyclooctadiene, cyclooctene, 2,4,6-tri-*tert*-butylphenol, trityl chloride, zinc powder, tetrabutylammonium chloride and ferrocinium hexafluorophosphate were purchased from Aldrich. All C-H substrates were dried over calcium hydride and distilled under nitrogen or vacuum. Aryl azides were synthesized following published literature procedures: 3,5-bis(trifluoromethyl)phenyl azide[2], 2,6-diisopropylphenyl azide[3], 4-nitro and 4-methoxyphenyl azide[4]. Gomberg's dimer was synthesized following previously reported procedure.[5] Celite® 545 (J. T. Baker) was dried in a Schlenk flask for 24 h under dynamic vacuum while heating to at least 150 °C prior to use in a drybox. Silica gel 32-63 μ (AIC, Framingham, MA) was used as received.

Characterization and Physical Measurements. ^{1}H, ^{13}C, and ^{19}F NMR spectra were recorded on Varian Unity/Inova 400 or 500 MHz- spectrometers. ^{1}H and ^{13}C NMR chemical shifts are reported relative to $SiMe_4$ using the chemical shift of residual solvent peaks as reference. ^{19}F NMR chemical shifts are reported relative to an external standard of boron trifluoride diethyl etherate. Gas chromatography/mass spectrometry (GC/MS) was performed on an Agilent GC/MS 5975 Turbo system. High-resolution mass spectrometry was performed on a Bruker microTOFII ESI LCMS or Bruker Maxis Impact LC-q-TOF Mass Spectrometer. Elemental analyses were carried out by Complete Analysis Laboratories, Inc. (Parsippany, NJ).

---

[1] Hennessy, E. T.; Liu, R. Y.; Iovan, D. A.; Duncan, R. A.; Betley, T. A. *Chem. Sci.* **2014**, *5*, 1526.
[2] Laitar , D. S.; Mathison , C. J. N.; Davis, W. M.; Sadighi, J. P. *Inorg. Chem.* **2003**, *42*, 7354.
[3] Guisado-Barrios, G.; Bouffard, J.; Donnadieu, B.; Bertrand, G. *Angew. Chem Int.Ed.* **2010**, *49*, 4759.
[4] Smith, P. A. S.; Hall, J. H. *J. Am. Chem. Soc.* **1962**, *84*, 480.
[5] Jang, E. S.; McMullin, C. L.; Käß, M.; Meyer, K.; Cundari, T. R.; Warren, T. H. *J. Am. Chem. Soc.* **2014**, *136*, 10930

Zero-field ^{57}Fe Mössbauer spectra were measured with a constant acceleration spectrometer (SEE Co, Minneapolis, MN) at 90 K. Isomer shifts are quoted relative to Fe foil at room temperature. Data was analyzed and simulated with Igor Pro 6 software (WaveMetrics, Portland, OR) using Lorentzian fitting functions. Samples were prepared by suspending 25-50 mg of compound in sufficient Paratone oil and immobilizing by rapid freezing in liquid nitrogen.

EPR spectra were obtained on a Bruker EleXsys E-500 CW-EPR spectrometer. Spectra were measured as frozen toluene glasses at a microwave power of 0.6325–2 mW. Spectral simulations incorporating spin state and rhombicity were performed using VisualRhombo.[6]

Magnetic data were collected using a Quantum Design MPMS-5S SQUID magnetometer. Measurements were obtained for finely ground microcrystalline powders restrained in a frozen eicosane matrix within polycarbonate capsules. Samples were prepared under a dry nitrogen atmosphere by packing the powder in a gelcap and adding warm liquid eicosane, which formed a solid wax upon cooling. Dc susceptibility measurements were collected in the temperature range 5-300 K under a dc field of 1000, 5000 or 10000 Oe. Dc magnetization measurements were obtained in the temperature range 1.8 – 10 K under dc fields of 1, 2, 3, 4, 5, 6, and 7 T. The susceptibility data was corrected for contributions from the sample holder and eicosane, as well as the core diamagnetism of the sample using Pascal's constants.

$$\chi_m = \frac{\chi M}{mH} \tag{S.1}$$

Molar susceptibilities were calculated from (χ_{m}) by converting the calculated magnetic susceptibility (χ) obtained from the magnetometer according to Eq. S.1. The reduced magnetization data were fit using PHI.[7]

[6] Hagen, W. R. *Mol. Phys.* **2007**, *105*, 2031–2039.
[7] Chilton, N. F.; Anderson, R. P.; Turner, L. D.; Soncini, A.; Murray, K. S. *J. Comput. Chem.* **2013**, *34*, 1164–1175.

Metal Complexes Syntheses.

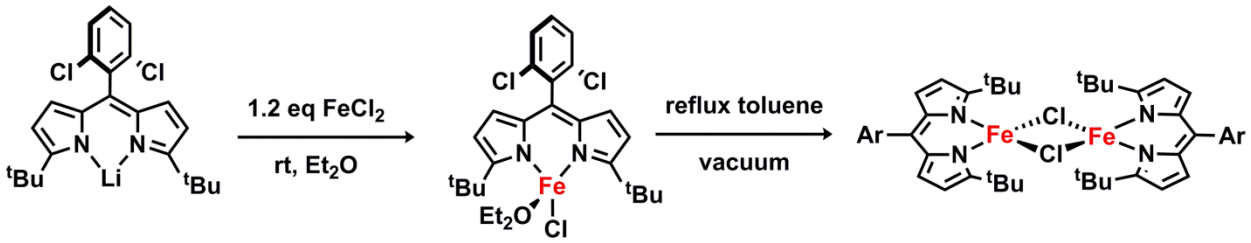

(**1**) (**2**)

[(^tBuL)FeCl]$_2$ (2): A solution of (**^tBuL)FeCl(OEt$_2$)** synthesized as previously reported[1] was refluxed in toluene for 30 min. The solvent was then removed under vacuum while heating and the resulting powder was collected in benzene and lyophilized to afford **[(^tBuL)FeCl]$_2$** as a green-brown microcrystalline powder (825 mg, 62 %, based on 1.1 g of (^{tBu}L)Li). Crystals suitable for X-ray diffraction were grown from a benzene solution at room temperature. **^{1}H NMR** (500 MHz, C_6D_6): δ 64.93 (br. s), 8.63 (s), 6.58 (m), 1.28(s), -12.26 (br. s). Anal. Calc. for $C_{46}H_{50}Cl_6Fe_2N_4$: C 56.19, H 5.13, N 5.70; Found C 55.98, H 5.23, N 5.61. Zero-field ^{57}Fe Mössbauer (90 K) δ = 0.94 mm/s, $|\Delta E_Q|$ = 1.96 mm/s. μ_{eff} (295 K, SQUID) 7.2 μ_B.

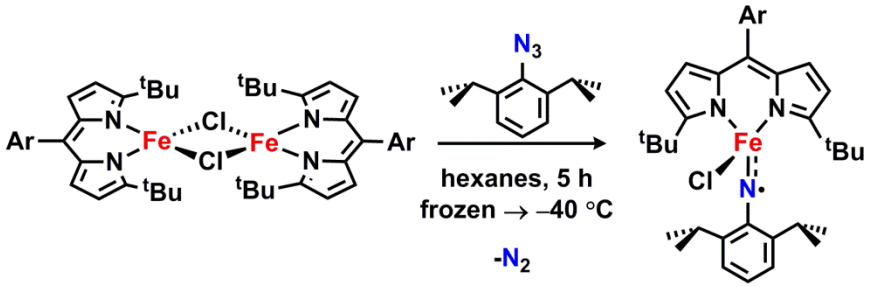

(**2**) (**3**)

(^tBuL)FeCl(^•NC$_6$H$_3$-2,6-^iPr$_2$) (3): Solid [(^{tBu}L)FeCl]$_2$ (**2**) (56.3 mg, 0.0573 mmol) was added to a frozen solution of 2,6-diisopropylphenyl azide (34.1 mg, 0.1677 mmol) in 3.1 g hexanes. The reaction mixture was warmed to –40 °C and allowed to stir at this temperature for 5 hours, during which time the color changed from pink-red to dark-red. The solution was filtered through Celite to remove unreacted [(^{tBu}L)FeCl]$_2$ and the solid collected was washed with 20 mL of cold hexanes. The solvent was removed *in vacuo* at –40 °C to afford green microcrystalline powder which was dissolved in minimal pentane and placed in the freezer at –35 °C overnight. The solution was decanted to remove excess azide and the solid was washed with cold pentane

and dried *in vacuo* to afford (**^{tBu}L)FeCl($^{\bullet}$NC$_6$H$_3$-2,6-^{i}Pr$_2$)** as a dark green microcrystalline powder (28.4 mg, 38 %). Crystals suitable for X-ray diffraction were grown from a solution of fluorobenzene layered with pentane at –35 °C. **^{1}H NMR** (500 MHz, C_6D_6): δ 70.99 (br. s), 65.26 (br. s), 30.00 (br. s), (20.30 (br. s), 1.12 (s). Anal. Calc. for $C_{35}H_{42}Cl_3FeN_3$: C 63.03, H 6.35, N 6.30; Found C 62.89, H 6.20, N 6.17. Zero-field ^{57}Fe Mössbauer (90 K) δ = 0.37 mm/s, $|\Delta E_Q|$ = 2.17 mm/s. μ_{eff} (295 K, SQUID) 4.7 μ_B.

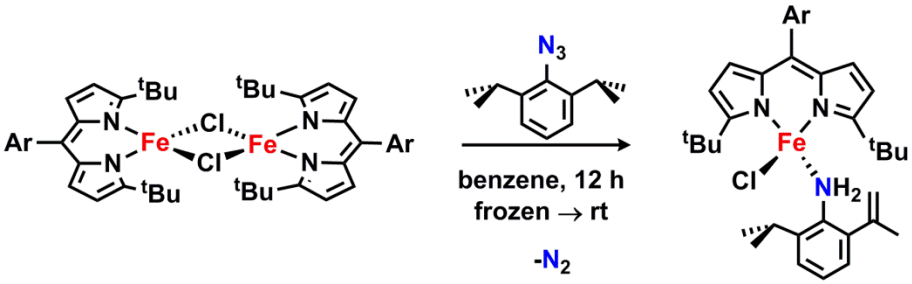

(**2**) (**4**)

(^{tBu}**L)FeCl(H$_2$N(C$_6$H$_3$-2-^{i}Pr-6-C(CH$_2$)(CH$_3$))) (4):** A thawing solution of [(^{tBu}L)FeCl]$_2$ (**2**) in 2 mL of benzene (30.6 mg, 0.0311 mmol) was added to a frozen solution of 2,6-diisopropylphenyl azide (12.9 mg, 0.0635 mmol) in 0.8 mL of benzene and the reaction was allowed to stir while warming to room temperature. After 12 hours, the solvent was removed *in vacuo* to afford **(**^{tBu}**L)FeCl(H$_2$N(C$_6$H$_3$-2-^{i}Pr$_2$-6-C(CH$_2$)(CH$_3$)))** as a dark green solid. Crystals suitable for X-ray diffraction were grown from a 1:2 solution of benzene:hexanes at –35 °C. **^{1}H NMR** (500 MHz, C_6D_6): δ 59.54 (br. s), 18.81 (br. s), 13.35(br. s), 9.82 (s), 8.82 (s), 3.01 (s), -2.17 (s), -7.56 (br. s). Anal. Calc. for $C_{35}H_{42}Cl_3FeN_3$: C 63.03, H 6.35, N 6.30; Found C 62.91, H 6.03, N 6.21. Zero-field ^{57}Fe Mössbauer (90 K) 70% δ = 0.95 mm/s, $|\Delta E_Q|$ = 3.16 mm/s; 30% δ = 0.99 mm/s, $|\Delta E_Q|$ = 2.29 mm/s.

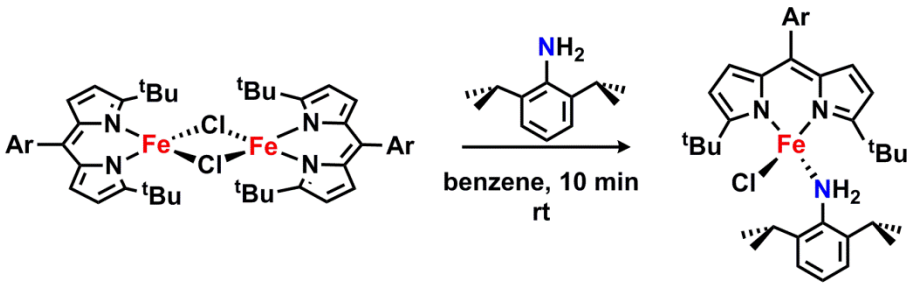

(**2**) (**5**)

(^{tBu}L)FeCl($H_2NC_6H_3$-2,6-^{i}Pr$_2$) (5): A solution of 2,6-diisopropylaniline in benzene was added to a solution of [(^{tBu}L)FeCl]$_2$ (**2**) in benzene and the reaction was stirred for 10 min at room temperature. Solvent was removed *in vacuo* to afford **(^{tBu}L)FeCl($H_2NC_6H_3$-2,6-^{i}Pr$_2$)** quantitatively as a dark red powder. **^{1}H NMR** (500 MHz, C_6D_6): δ 56.72 (br. s), 36.87(br. s), 18.95 (br. s), 10.42 (s), 7.83 (s), -0.11 (s), -4.59 (br. s), - 7.29 (br. s), -10.09 (br. s). Anal. Calc. for $C_{35}H_{44}Cl_3FeN_3$: C 62.84, H 6.63, N 6.28; Found C 62.74, H 6.62, N 6.19. Zero-field ^{57}Fe Mössbauer (90 K) δ = 0.92 mm/s, $|\Delta E_Q|$ = 2.91 mm/s.

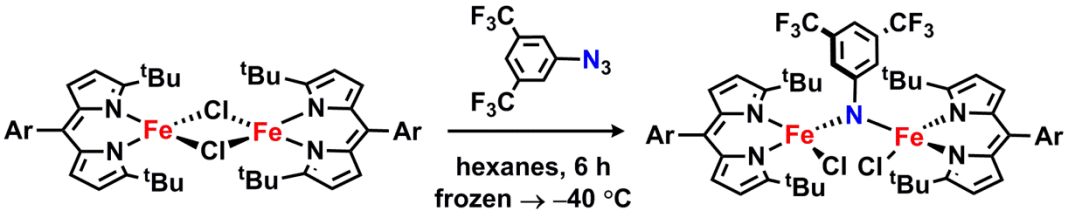

[(^{tBu}L)FeCl]$_2$(μ-NC_6H_3-3,5-(CF_3)$_2$) (6): Solid [(^{tBu}L)FeCl]$_2$ (**2**) (69.4 mg, 0.0706 mmol) was added to a frozen solution of 3,5-bis(trifluoromethyl)phenyl azide (90.8 mg, 0.3601 mmol) in hexanes. The reaction mixture was warmed to –40 °C and allowed to stir at this temperature for 6 hours, during which time the color changed from red to brown. The solution was filtered through Celite and the solid was washed with cold pentane to remove excess azide. The solid was collected in benzene and solution lyophilized to afford **[(^{tBu}L)FeCl]$_2$(μ-NC_6H_3-3,5-(CF_3)$_2$)** as a dark-green powder (41.9 mg, 49 %). Crystals suitable for X-ray diffraction were grown from a 1:2 solution of benzene:hexanes at –35 °C. **^{1}H NMR** no resonances. **^{19}F NMR** (470 MHz, C_6D_6): δ -67.03 ppm. Anal. Calc. for $C_{54}H_{53}Cl_6F_6Fe_2N_5$: C 53.58, H 4.41, N 5.79; Found C 53.38, H 4.55, N 5.73.Zero-field ^{57}Fe Mössbauer (90 K) δ = 0.33 mm/s, $|\Delta E_Q|$ = 1.48 mm/s. μ_{eff} (295 K, SQUID) 3.1 μ_B.

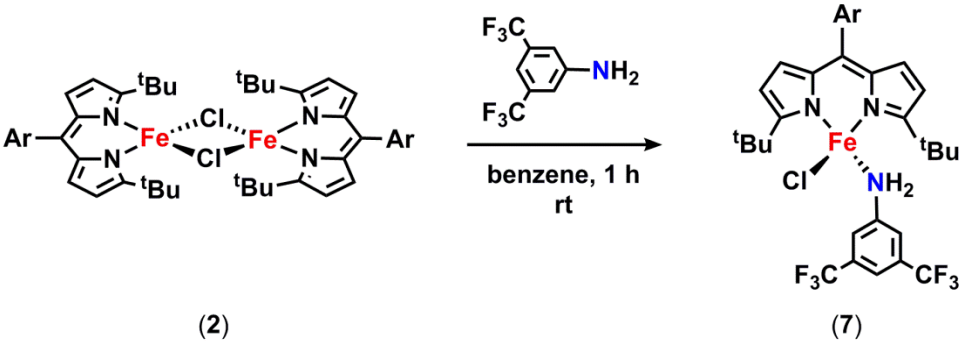

(^{tBu}L)FeCl($H_2NC_6H_3$-3,5-$(CF_3)_2$) (7): A solution of 3,5-bis(trifluoromethyl)aniline (23.3 mg, 0.1017 mmol) in 5 mL of benzene was added to [(^{tBu}L)FeCl]$_2$ (**2**) (50 mg, 0.0508 mmol) and the reaction was allowed to stir for 1 hour at room temperature, during which color changed from pink-red to dark red. Solvent was removed *in vacuo* to afford **(^{tBu}L)FeCl($H_2NC_6H_3$-3,5-$(CF_3)_2$)** as a red-brown powder quantitatively. Crystals suitable for X-ray diffraction were grown from a solution of hexanes with drops of benzene at –35 °C. **^{1}H NMR** (500 MHz, C_6D_6): δ 60.47(br. s), 21.54 (br. s), 11.91 (s), 10.63 (s), 7.01 (s), 3.52 (s), 1.59 (s), -2.73 (br. s), -16.13 (br. s). **^{19}F NMR** (470 MHz, C_6D_6): δ -66.3 ppm. Anal. Calc. for $C_{31}H_{30}Cl_3F_6FeN_3$: C 51.66, H 4.20, N 5.83; Found C 51.55, H 4.32, N 6.01. Zero-field ^{57}Fe Mössbauer (90 K) δ = 0.92 mm/s, $|\Delta E_Q|$ = 2.41 mm/s.

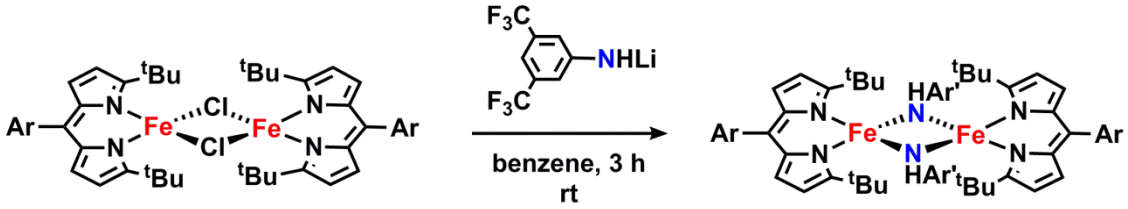

(**2**) (**8**)

[(^{tBu}L)Fe(HNC_6H_3-3,5-$(CF_3)_2$)]$_2$ (8): A thawing solution of [(^{tBu}L)FeCl]$_2$ (**2**) (99.7 mg, 0.1014 mmol) in 5 mL of benzene was added to a frozen slurry of lithium 3,5-bis(trifluoromethyl)anilide (47.5 mg, 02021 mmol) in 0.5 mL of benzene and the reaction was allowed to thaw and stir at room temperature for 3 hours. The solution was filtered through Celite to remove lithium chloride and concentrated *in vacuo*. The resulting solid was dissolved in minimal pentane and placed in the freezer at –35 °C overnight. Solvent was decanted and the dark-red powder dried *in vacuo* to afford **[(^{tBu}L)Fe(HNC_6H_3-3,5-$(CF_3)_2$)]$_2$** (97.7 mg, 74 %). Crystals suitable for X-ray diffraction were grown from a solution of pentane at –35 °C. **^{1}H NMR** (500 MHz, C_6D_6): δ 70.64 (s), 19.81 (s), 7.75 (s), 6.74 (s), 1.14 (s), -78.31 (s). **^{19}F NMR** (470 MHz, C_6D_6): δ -93.0 ppm. Anal. Calc. for $C_{62}H_{58}Cl_4F_{12}Fe_2N_6$: C 54.41, H 4.27, N 6.14; Found C 54.09, H 4.32, N 5.84. Zero-field ^{57}Fe Mössbauer (90 K) 67 % δ = 0.90 mm/s, $|\Delta E_Q|$ = 2.29 mm/s; 33 % δ = 0.64 mm/s, $|\Delta E_Q|$ = 0.75 mm/s. Addition of pyridine to **8** affords the four-coordinate pyridine adduct which displays a zero-field ^{57}Fe Mössbauer (90 K) δ = 0.86 mm/s, $|\Delta E_Q|$ = 2.9 mm/s (Figure S-10), suggesting that the two quadrupole doublets observed in the spectrum of **8** are indicative of a mixture of monomer and dimer, both of which convert to the four-coordinate species upon

addition of a coordinating solvent, pyridine (Figure S-11). **^{1}H NMR** (500 MHz, C_6D_6): δ 45.13 (s), 13.18 (s), 8.77 (s), 5.47 (s), 1.30 (s), -68.30 (s). **^{19}F NMR** (470 MHz, C_6D_6): δ -86.09 ppm.

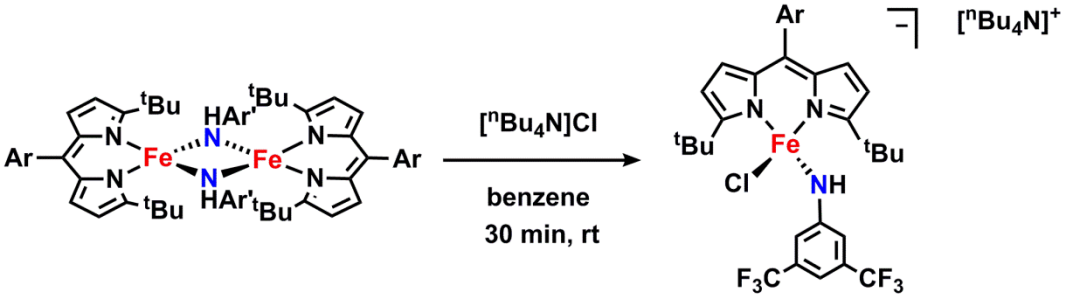

(**8**) (**12**)

[(^{tBu}L)FeCl(HNC$_6$H$_3$-3,5-(CF$_3$)$_2$)][^{n}Bu$_4$N] (12): A solution of [(^{tBu}L)Fe(HNC$_6$H$_3$-3,5-(CF$_3$)$_2$)]$_2$ (**8**) (60 mg, 0.0438 mmol) in 5 mL of benzene was added to a slurry of tetrabutylammonium chloride (26.2 mg, 0.0936 mmol) in 0.5 mL of benzene and reaction was allowed to stir at room temperature for 30 min, during which color changed from red to brown-orange. Solution was filtered through Celite and solvent removed *in vacuo*. The resulting solid was triturated with hexanes three times, dried *in vacuo*, dissolved in benzene and solution lyophilized to afford **[(^{tBu}L)FeCl(HNC$_6$H$_3$-3,5-(CF$_3$)$_2$)][^{n}Bu$_4$N]** as a brown-orange solid (77.9 mg, 92 %). **^{1}H NMR** (500 MHz, C_6D_6): δ 47.49 (s), 16.66 (br. s), 13.32 (br. s), 5.08 (s), 4.63 (s), 3.08 (s), 2.30 (s), 1.81 (s), 1.13 (s), -8.28 (s), -61.93 (s). **^{19}F NMR** (470 MHz, C_6D_6): δ -76.7, -85.9. Zero-field ^{57}Fe Mössbauer (90 K) δ = 0.92 mm/s, $|\Delta E_Q|$ = 3.29 mm/s. Anal. Calc. for $C_{50}H_{72}Cl_3F_6FeN_4$: C 59.74, H 7.22, N 5.57; Found C 59.78, H 7.34, N 5.67. Zero-field ^{57}Fe Mössbauer (90 K) δ = 0.92 mm/s, $|\Delta E_Q|$ = 3.29 mm/s. **HRMS** (ESI$^+$) *m/z* Calc. 718.0687 $[C_{31}H_{29}Cl_3F_6FeN_3]^+$, Found. 718.0696 $[M]^+$.

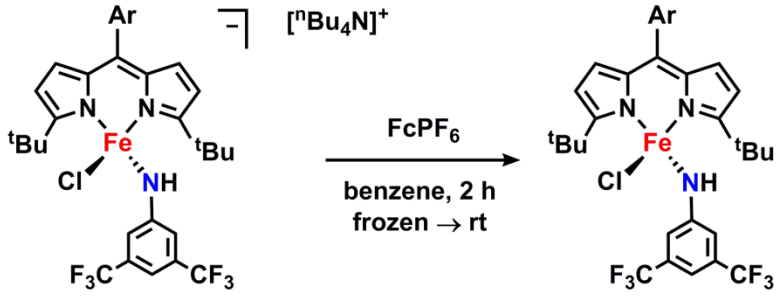

(**12**) (**9**)

(^{tBu}L)FeCl(HNC$_6$H$_3$-3,5-(CF$_3$)$_2$) (9): A thawing solution of [(^{tBu}L)FeCl(HNC$_6$H$_3$-3,5-(CF$_3$)$_2$)][^{n}Bu$_4$N] (**12**) (77.9 mg, 0.0810 mmol) in 5 mL benzene was added to a frozen slurry of ferrocinium hexafluorophosphate (40.1 mg, 0.1211 mmol) in 1 mL of benzene and the mixture was allowed to thaw and stir at room temperature for 2 hours during which the color changed from brown-orange to dark brown. The reaction was filtered through Celite to remove insoluble salts and the solvent removed *in vacuo* to afford **(^{tBu}L)FeCl(HNC$_6$H$_3$-3,5-(CF$_3$)$_2$)** as a brown powder. The solubility of the iron complex in pentane prevented removal of ferrocene. Additionally, attempts to sublime the ferrocene away by heating the iron complex under vacuum led to decomposition. As such, the yield is reported by accounting for 100 % recovery of the corresponding amount of ferrocene upon oxidation (78 %). **^{1}H NMR** (500 MHz, C_6D_6): δ 94.16 (br. s), 30.54 (br. s), 25.86 (br. s), 1.28 (s), 0.10 (s). **^{19}F NMR** (470 MHz, C_6D_6): δ -148.1 ppm. Anal. Calc. for $C_{41}H_{39}Cl_3F_6Fe_2N_3$ (^{tBu}LFeCl(NHC$_6$H$_3$-3,5-(CF$_3$)$_2$) + ferrocene): C 54.37, H 4.34, N 4.64; Found C 54.43, H 4.20, N 4.53. Zero-field ^{57}Fe Mössbauer (90 K) δ = 0.29 mm/s, $|\Delta E_Q|$ = 1.22 mm/s. EPR (toluene, 77 K): g_{eff} = 8.52, 5.39, 2.99.

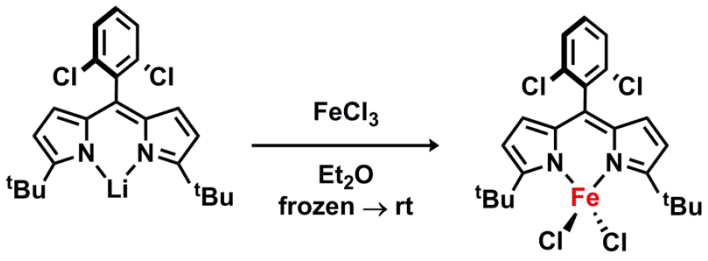

(**10**)

(^{tBu}L)FeCl$_2$ (10): A thawing solution of $FeCl_3$ (79.7 mg, 0.914 mmol) in 2 mL of diethyl ether was added to a frozen solution of (^{tBu}L)Li (200 mg, 0.4924 mmol) in 8 mL of diethyl ether and the mixture was allowed to warm to room temperature and stir overnight, during which color changed from yellow to brown-green. The reaction was filtered through Celite and solvent was removed *in vacuo*. The resulting residue was collected in hexanes (100 mL), filtered through Celite and the solvent removed *in vacuo*. The solids were collected in minimal benzene and solution lyophilized to afford **(^{tBu}L)FeCl$_2$** as a dark green powder (101 mg, 39 %). Crystals suitable for X-ray diffraction were grown from a solution of diethyl ether at –35 °C. **^{1}H NMR** (500 MHz, C_6D_6): δ 31.61 (br. s), 1.26 (s). Anal. Calc. for $C_{23}H_{25}Cl_4FeN_2$: C 52.41, H 4.78, N 5.31; Found C 52.28, H 4.67, N 5.15. Zero-field ^{57}Fe Mössbauer (90 K) δ = 0.19 mm/s, $|\Delta E_Q|$ = 0.51 mm/s. EPR (toluene, 77 K): g_{eff} = 8.45, 5.43, 2.95.

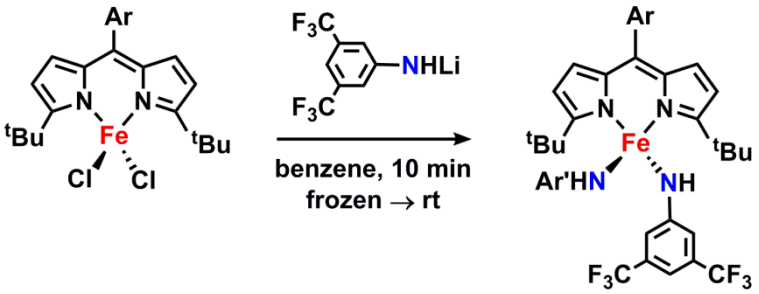

(**10**) (**11**)

(^{tBu}L)Fe(HNC$_6$H$_3$-3,5-(CF$_3$)$_2$)$_2$ (11): Solid (^{tBu}L)FeCl$_2$ (**10**) (40 mg, 0.0759 mmol) was added to a frozen slurry of lithium 3,5-bis(trifluoromethyl)anilide (24.5 mg, 0.1042 mmol) in 7 mL of benzene and reaction was allowed to thaw and stir at room temperature for 10 min, during which color changed from brown-green to purple. Solution was filtered through Celite to remove insoluble salts and solvent was removed *in vacuo* to afford **(^{tBu}L)Fe(HNC$_6$H$_3$-3,5-(CF$_3$)$_2$)$_2$** as a dark purple powder (61.4 mg, 89 %). Crystals suitable for X-ray diffraction were grown from a solution of toluene layered with hexanes at –35 °C. **^{1}H NMR** (500 MHz, C_6D_6): δ 92.35 (br. s), 26.11 (br. s), 19.96 (br. s), 1.28 (s), 0.10 (s). **^{19}F NMR** (470 MHz, C_6D_6): δ -128.0 ppm. Anal. Calc. for $C_{39}H_{33}Cl_2F_{12}FeN_4$: C 51.34, H 3.65, N 6.14; Found C 51.31, H 3.59, N 6.04. Zero-field ^{57}Fe Mössbauer (90 K) δ = 0.25 mm/s, $|\Delta E_Q|$ = 1.18 mm/s. EPR (toluene, 77 K): g_{eff} = 7.7, 5.7, 4.1.

Stoichiometric Reactions

For zero-field ^{57}Fe Mössbauer analysis:

Under an inert N_2 atmosphere, a thawing solution of [(^{tBu}L)FeCl]$_2$ (**2**) in 2 mL of benzene was added to a frozen solution of the desired azide (1 equiv) in 0.5 mL of benzene. The resultant solution was allowed to thaw and stir at room temperature for 5 min. The reaction mixture was then lyophilized and the powder was analyzed via zero-field ^{57}Fe Mössbauer spectroscopy.

For ^{1}H and ^{19}F NMR analysis:

Under an inert N_2 atmosphere, a solution of [(^{tBu}L)FeCl]$_2$ (**2**) in 0.5 mL of benzene-d_6 was layered onto a frozen solution of the desired azide (1 equiv) in 0.3 mL of benzene-d_6 into an nmr tube. The reaction was thawed immediately prior to acquisition of the spectrum.

For EPR analysis:

Under an inert N_2 atmosphere, a thawing solution of [(^{tBu}L)FeCl]$_2$ (**2**) in 1 mL of benzene was added to a frozen solution of the 3,5-bis(trifluoromethyl)phenyl azide (1 equiv) in 0.5 mL of benzene. Immediately upon thawing, an aliquant of the reaction was diluted with toluene, transferred to an epr tube and frozen in liquid N_2 for spectra acquisition. This was repeated at different time points during the reaction.

Catalytic Reactions

Allylic C-H bond amination

Under an inert N_2 atmosphere, a solution of $[(^{tBu}L)FeCl]_2$ (**2**) (7.0 mg, 0.0071 mmol) in the desired C-H substrate (0.5 mL) was added to a frozen solution of the 3,5-bis(trifluoromethyl)phenyl azide (36.3, 0.144 mmol) in the desired C-H substrate (0.2 mL). The reaction was allowed to thaw and stir at room temperature for 12 hours. The solution was concentrated *in vacuo* to remove excess substrate and product was isolated via silica gel column chromatography using hexanes as eluent. Average yields of two or three runs are reported.

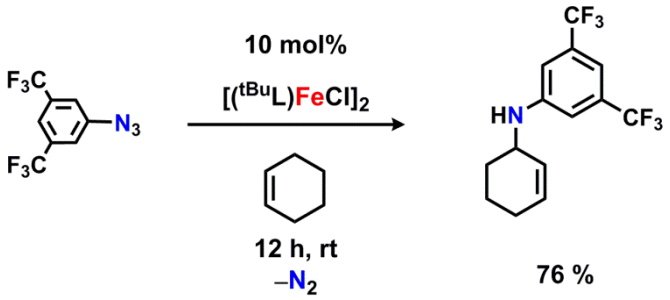

Formation of *N*-(cyclohex-2-en-1-yl)-3,5-bis(trifluoromethyl)aniline upon reaction with cyclohexene was confirmed via ^{1}H and ^{19}F NMR and GC-MS. Spectral data were consistent with previously reported characterization of the product.[8]

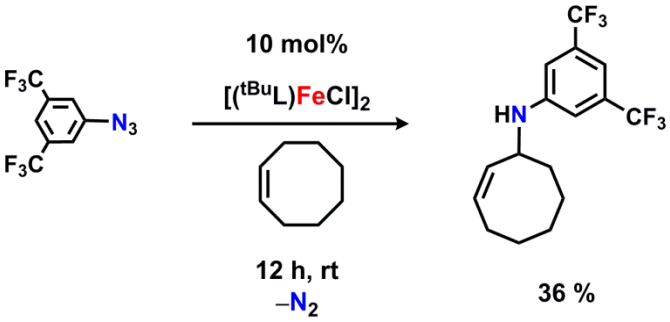

(Z)-*N*-(3,5-bis(trifluoromethyl)phenyl)cyclooct-2-en-1-amine: ^{1}H NMR (500 MHz, $CDCl_3$) δ 7.13 (s, 1 H), 6.88 - 6.97 (s, 2 H), 5.88 (q, *J*=8.79 Hz, 1 H), 5.23 - 5.37 (m, 1 H), 4.09 - 4.33 (m, 2 H), 2.18 - 2.38 (m, 2 H), 1.91 - 2.03 (m, 1 H), 1.36 - 1.86 (m, 7 H). **^{13}C NMR** (125 MHz, $CDCl_3$) δ 148.3, 133.2, 132.2 (q, J_{C-F} = 32.5 Hz), 131.9, 123.6 (q, J_{C-F} = 268.8 Hz), 112.23, 109.9, 50.8, 36.3, 29.7, 26.9, 26.6, 24.2. **^{19}F NMR** (376 MHz, $CDCl_3$) δ -63.06. **HRMS** (ESI^+)

[8] Haubenreisser, S.; Niggemann, M. *Adv. Synth. Catal.* **2011**, *353*, 469.

m/z Calc. 338.1343 $[C_{16}H_{17}F_6N+H]^+$, Found. 338.1336 $[M+H]^+$. **GCMS** (EI) t_R = 8.958 min *m/z*: 53, 67, 79, 93, 109, 125, 144, 163, 185, 198, 213, 229, 2422, 255, 268, 281, 294, 318, 337.

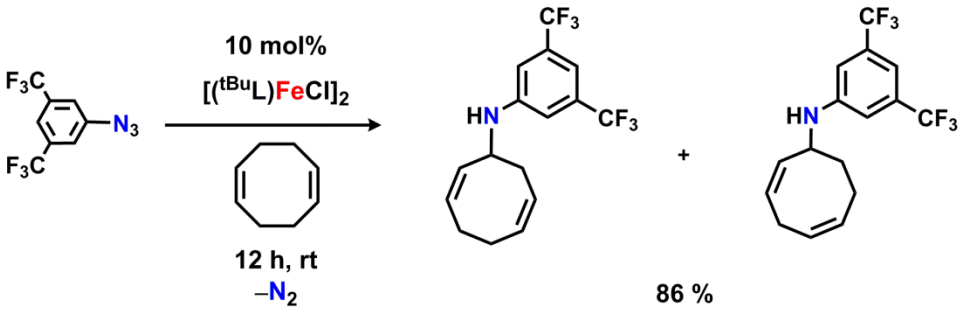

(2Z,6Z)-*N*-(3,5-bis(trifluoromethyl)phenyl)cycloocta-2,6-dien-1-amine (a) and (2Z,5Z)-N-(3,5-bis(trifluoromethyl)phenyl)cycloocta-2,5-dien-1-amine (b): ^{1}H NMR (500 MHz, $CDCl_3$) δ 7.16 (s, 1 H, **a**), 7.14 (s, 0.6 H, **b**), 6.97 (s, 2 H, **a**), 6.94 (s, 1.2 H, **b**), 5.89 - 5.94 (m, 0.6 H, **b**), 5.67 - 5.79 (m, 2.6 H, **a** and **b**), 5.52 - 5.63 (m, 1.6 H, **a** and **b**), 5.39 - 5.45 (m, 1 H, **a**), 5.11 - 5.18 (m, 0.6 H, **b**), 4.68 (br. s., 1 H, **a**), 4.59 (br. s., 0.6 H, **b**), 4.23 (br. s., 0.6 H, **b**), 4.15 (d, *J*=5.86 Hz, 1 H, **a**), 2.97 - 3.03 (m, 1.2 H, **b**), 2.71 - 2.85 (m, 1.6 H, **a** and **b**), 2.54 - 2.65 (m, 2 H, **a**), 2.31 - 2.44 (m, 2 H,), 2.20 - 2.30 (m, 1 H, **a**), 2.06 - 2.14 (m, 0.6 H, **b**), 1.91 (tt, *J*=12.45, 4.88 Hz, 0.6 H, **b**), 1.39 - 1.47 (m, 0.6 H, **b**). **^{13}C NMR** (125 MHz, $CDCl_3$) δ 148.3, 147.7, 132.7, 132.4 (q, $J_{C\text{-}F}$ = 32.5 MHz), 132.2 (q, $J_{C\text{-}F}$ = 32.5 MHz), 131.3, 130.4, 130.3, 130.1, 129.9, 128.1, 125.0, 123.6 (q, $J_{C\text{-}F}$ = 270 MH), 123.5 (q, $J_{C\text{-}F}$ = 270 MH), 112.4, 112.2, 110.2, 110.0, 52.5, 51.0, 33.8, 29.9, 29.7, 28.5, 27.4, 23.1. **^{19}F NMR** (376 MHz, $CDCl_3$) δ -63.05 (**a**), -63.08 (**b**). **HRMS** (ESI^+) *m/z* Calc. 336.1187 $[C_{16}H_{15}F_6N+H]^+$, Found. 336.1186 $[M+H]^+$. **GCMS** (EI) **a**: t_R = 8.935 min *m/z*: 53, 68, 91, 105, 125, 144, 163, 185, 198, 213, 240, 260, 281, 294, 316, 335; **b**: t_R = 8.855 min *m/z*: 51, 65, 79, 91, 107, 125, 144, 163, 185, 198, 213, 240, 254, 268, 281, 294, 307, 316, 320, 335.

Toluene amination

Under an inert N_2 atmosphere, a solution of $[(^{tBu}L)FeCl]_2$ (**2**) (7.0 mg, 0.0071 mmol) in toluene (0.5 mL) was added to a frozen solution of the 3,5-bis(trifluoromethyl)phenyl azide (36.3, 0.144 mmol) in toluene (0.2 mL). The reaction was allowed to thaw and stir at room temperature for 12 hours. The solution was concentrated *in vacuo* to remove excess toluene and residue was loaded onto a neutral alumina gel eluting with a 10:1 mixture of dichloromethane and methanol to remove paramagnetic materials. A known amount of ferrocene was added as an internal standard

prior to removal of solvent under vacuum. Formation of *N*-benzyl-3,5-bis(trifluoromethyl)aniline was confirmed via ^{1}H and ^{19}F NMR and GC-MS. Spectral data were consistent with previously reported characterization of the product.[9] Yield is reported by integration versus the internal standard ferrocene.

Styrene aziridination

Under an inert N_2 atmosphere, a solution of $[(^{tBu}L)FeCl]_2$ (**2**) (7.0 mg, 0.0071 mmol) in styrene (0.5 mL) was added to a frozen solution of the 3,5-bis(trifluoromethyl)phenyl azide (37.1 mg, 0.1471 mmol) in styrene (0.2 mL). The reaction was allowed to thaw and stir at room temperature for 1 hour. Full consumption of azide was confirmed via ^{19}F NMR. The solution was concentrated *in vacuo* to remove excess styrene. 10 μL of 1,2-difluorobenzene was added as standard to determine the amount of product formed.

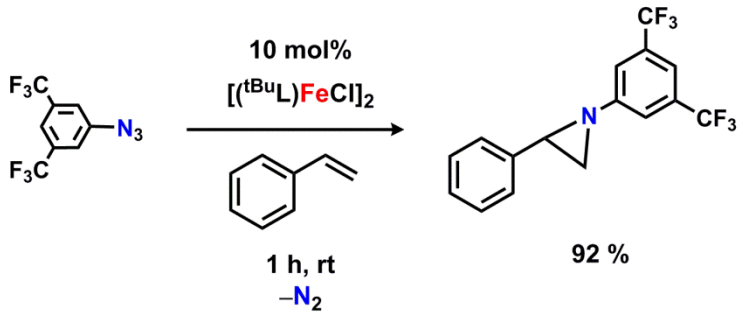

Formation of 1-(3,5-bis(trifluoromethyl)phenyl)-2-phenylaziridine upon reaction with styrene was confirmed via ^{1}H and ^{19}F NMR and GC-MS. Spectral data were consistent with previously reported characterization of the product.[10]

[9] Cano, R.; Yus, M.; Ramón, D. J. *Tetrahedron* **2011**, *67*, 8079.

[10] Fantauzzi, S.; Gallo, E.; Caselli, A.; Piangiolino, C.; Ragaini, F.; Cenini, S. *Eur. J. Org. Chem.* **2007**, *36*, 6053.

Reactions of (^{tBu}L)FeCl($^{\bullet}$NC$_6$H$_3$-2,6-^{i}Pr$_2$) and [(^{tBu}L)FeCl]$_2$(μ-NC$_6$H$_3$-3,5-(CF$_3$)$_2$))

Reaction with 1,4-cyclohexadiene.

Excess 1,4-cyclohexadiene was added to a frozen solution of (^{tBu}L)FeCl($^{\bullet}$NC$_6$H$_3$-2,6-^{i}Pr$_2$) (**3**) or [(^{tBu}L)FeCl]$_2$(μ-NC$_6$H$_3$-3,5-(CF$_3$)$_2$) (**6**) in 1 mL benzene-d_6. The reaction mixture was warmed to room temperature and the ^{1}H NMR showed resonances consistent with formation of the corresponding iron(II) aniline adducts (^{tBu}L)FeCl(H$_2$NC$_6$H$_3$-2,6-^{i}Pr$_2$) (**5**) and (^{tBu}L)FeCl(H$_2$NC$_6$H$_3$-3,5-(CF$_3$)$_2$) (**7**), respectively.

Reaction with cyclohexene.

A solution of (^{tBu}L)FeCl($^{\bullet}$NC$_6$H$_3$-2,6-^{i}Pr$_2$) (**3**) in cyclohexene was allowed to stir at room temperature for 12 hours under an inert N_2 atmosphere. The reaction was removed from the glove box, concentrated *in vacuo* and ran through a neutral alumina gel eluting with a 10:1 mixture of dichloromethane and methanol to remove paramagnetic materials. ^{1}H NMR and GC-MS revealed formation of 2-isopropyl-6-(prop-1-en-2-yl)aniline as the dominant species and no C-H amination of cyclohexene was observed.

Reaction of [(^{tBu}L)FeCl]$_2$(μ-NC$_6$H$_3$-3,5-(CF$_3$)$_2$)) with C-H substrates. A solution of [(^{tBu}L)FeCl]$_2$(μ-NC$_6$H$_3$-3,5-(CF$_3$)$_2$) (**6**) in the desired C-H substrate was prepared in an nmr tube under an inert N_2 atmosphere. The ^{19}F NMR showed consumption of starting material and formation of the expected functionalized product. Upon removal of the C-H substrate under vacuum, samples were checked by GC-MS to confirm the formation of the desired products.

Reactions with 2,4,6-tri-*tert*-butylphenol

A: A thawing solution of [(^{tBu}L)FeCl]$_2$ (**2**) (35 mg, 0.0356 mmol) and 2,4,6-tri-*tert*-butylphenol (18.7 mg, 0.0712 mmol) in 3 mL of benzene was added to a frozen solution of 3,5-bis(trifluoromethyl)phenyl azide (18 mg, 0.0713 mmol). The reaction was allowed to thaw and stir at room temperature for 12 h. The solvent was removed *in vacuo* and resulting powder was analyzed via zero-field ^{57}Fe Mössbauer to confirm formation of (^{tBu}L)FeCl(HNC$_6$H$_3$-3,5-(CF$_3$)$_2$) (**9**). ^{19}F NMR revealed (^{tBu}L)FeCl(HNC$_6$H$_3$-3,5-(CF$_3$)$_2$) (**9**) as the dominant species. ^{1}H NMR showed resonances that were identified as the product of the reaction of [(^{tBu}L)FeCl]$_2$ (**2**) and 2,4,6-tri-*tert*-butylphenoxyl radical. Frozen solution EPR collected at 77 K in toluene revealed signals consistent with (^{tBu}L)FeCl(HNC$_6$H$_3$-3,5-(CF$_3$)$_2$) (**9**).

B: A solution of 2,4,6-tri-*tert*-butylphenol (15.7 mg, 0.0598 mmol) in 2 mL of benzene was added to a pre-cooled vial containing [(^{tBu}L)FeCl]$_2$(μ-NC$_6$H$_3$-3,5-(CF$_3$)$_2$) (**6**) (35.5 mg). Upon warming to room temperature, the resulting dark brown solution was allowed to stir for 1 h. Solvent was removed *in vacuo*. ^{19}F NMR and frozen solution EPR (toluene, 77 K) revealed the formation of (^{tBu}L)FeCl(HNC$_6$H$_3$-3,5-(CF$_3$)$_2$) (**9**). A mixture of different iron-containing species were detected via zero-field ^{57}Fe Mössbauer spectroscopy, however, the broadness of the spectrum prevented any definitive assignments.

Synthesis of (^{tBu}L)Fe(HNC$_6$H$_3$-3,5-(CF$_3$)$_2$)$_2$ from [(^{tBu}L)Fe(HNC$_6$H$_3$-3,5-(CF$_3$)$_2$)]$_2$

Ligand exchange: Solutions of [(^{tBu}L)Fe(HNC$_6$H$_3$-3,5-(CF$_3$)$_2$)]$_2$ (**8**) and (^{tBu}L)FeCl(HNC$_6$H$_3$-3,5-(CF$_3$)$_2$) (**9**) in benzene were mixed to afford a dark purple reaction mixture. ^{19}F NMR revealed formation of (^{tBu}L)Fe(HNC$_6$H$_3$-3,5-(CF$_3$)$_2$)$_2$ (**11**) and resonances for [(^{tBu}L)FeCl]$_2$ (**2**) were detected in the ^{1}H NMR (Figure S-27).

Reaction with azide: Under an inert N_2 atmosphere, a solution of [(^{tBu}L)Fe(HNC$_6$H$_3$-3,5-(CF$_3$)$_2$)]$_2$ (**8**) in 0.5 mL of benzene-d_6 was frozen onto a frozen solution of 3,5-bis(trifluoromethyl)phenyl azide (1 equiv.) in 0.3 mL of benzene-d_6 into an nmr tube. The reaction was thawed immediately prior to acquisition of the spectrum. Formation of (^{tBu}L)Fe(HNC$_6$H$_3$-3,5-(CF$_3$)$_2$)$_2$ (**11**) was observed immediately in the ^{19}F NMR spectrum and we hypothesize that upon generation of an iron iminyl intermediate, rapid hydrogen atom abstraction takes place to afford (^{tBu}L)Fe(HNC$_6$H$_3$-3,5-(CF$_3$)$_2$)$_2$ (**11**). Frozen solution EPR (toluene, 77 K) revealed signals consistent with formation of (^{tBu}L)FeCl(HNC$_6$H$_3$-3,5-(CF$_3$)$_2$) (**11**) (Figure S-28).

Reactions of (^{tBu}L)FeCl(HNC$_6$H$_3$-3,5-(CF$_3$)$_2$) and (^{tBu}L)Fe(HNC$_6$H$_3$-3,5-(CF$_3$)$_2$)$_2$ with 1,4-cyclohexadiene.

A J. Young nmr tube was charged with a solution of (^{tBu}L)FeCl(HNC$_6$H$_3$-3,5-(CF$_3$)$_2$) (**9**) and (^{tBu}L)Fe(HNC$_6$H$_3$-3,5-(CF$_3$)$_2$)$_2$ (**11**) (generated upon addition of one equivalent of lithium 3,5-bis(trifluoromethyl)anilide to (^{tBu}L)FeCl$_2$ (**10**)) in benzene-d_6 and excess 1,4-cyclohexadiene was added. The tube was sealed under N_2 and the reaction mixture was heated to 65 °C. After 72 h, full consumption of (^{tBu}L)FeCl(HNC$_6$H$_3$-3,5-(CF$_3$)$_2$) (**9**) was observed via ^{19}F NMR and emergence of (^{tBu}L)FeCl(H$_2$NC$_6$H$_3$-3,5-(CF$_3$)$_2$) (**7**) was validated via both ^{19}F and ^{1}H NMR (Figure S-29). (^{tBu}L)Fe(HNC$_6$H$_3$-3,5-(CF$_3$)$_2$)$_2$ (**11**) did not react at this temperature. Independent treatment of (^{tBu}L)Fe(HNC$_6$H$_3$-3,5-(CF$_3$)$_2$)$_2$ (**11**) with excess 1,4-cyclohexadiene under identical conditions showed no consumption of starting material at 65 °C. Upon heating to 85 °C, formation of [(^{tBu}L)Fe(HNC$_6$H$_3$-3,5-(CF$_3$)$_2$)]$_2$ (**8**) was detected via both ^{19}F and ^{1}H NMR as well as other unidentified species, however, full consumption of the starting complex was not achieved.

Reactions of (^{tBu}L)FeCl(HNC$_6$H$_3$-3,5-(CF$_3$)$_2$) and (^{tBu}L)Fe(HNC$_6$H$_3$-3,5-(CF$_3$)$_2$)$_2$ with triphenylmethyl radical.

Under an inert N_2 atmosphere, a solution of (^{tBu}L)FeCl(HNC$_6$H$_3$-3,5-(CF$_3$)$_2$) (**9**) or (^{tBu}L)Fe(HNC$_6$H$_3$-3,5-(CF$_3$)$_2$)$_2$ (**11**) in 0.5 mL of benzene-d_6 was added to a solution of triphenylmethyl radical in benzene-d_6 and transferred to an nmr tube. Formation of the corresponding [(^{tBu}L)FeCl]$_2$ (**2**) (Figure S-30) and [(^{tBu}L)Fe(HNC$_6$H$_3$-3,5-(CF$_3$)$_2$)]$_2$ (**8**) (Figure S-31) was observed immediately in the ^{1}H and ^{19}F NMR spectra respectively. Upon full consumption of starting complexes, solutions were ran through a neutral alumina gel eluting with a 10:1 mixture of dichloromethane and methanol to remove paramagnetic materials. ^{1}H NMR revealed formation of 3,5-bis(trifluoromethyl)-*N*-tritylaniline which was independently synthesized for comparison.

3,5-bis(trifluoromethyl)-*N*-tritylaniline: Synthesized following previously reported procedure for tritylation of anilines[11], 61 % yield. **^{1}H NMR** (500 MHz, $CDCl_3$) δ 7.25 - 7.35 (m, 18 H), 7.04 (s, 1 H), 6.74 (s, 2 H), 5.47 (s, 1 H). **^{13}C NMR** (125 MHz, $CDCl_3$) δ 147.0, 144.0, 131.2 (q, $J_{C\text{-}F}$ = 32.5 MHz), 128.9, 128.3, 127.4, 123.3 (q, $J_{C\text{-}F}$ = 269 MHz), 115.1, 110.4, 71.8. **^{19}F NMR** (376 MHz, $CDCl_3$) δ -63.2 ppm. **GCMS** (EI) t_R = 15.132 min *m/z*: 470, 452, 394, 316, 281, 243, 228, 215, 188, 165, 139, 104, 77, 51.

Reactions of (^{tBu}L)FeCl(H$_2$NC$_6$H$_3$-3,5-(CF$_3$)$_2$) with 2,4,6-tri-*tert*-butylphenoxyl radical.

Under an inert N_2 atmosphere, a solution of (^{tBu}L)FeCl(H$_2$NC$_6$H$_3$-3,5-(CF$_3$)$_2$) (**7**) 0.5 mL of benzene-d_6 was added to a solution of 2,4,6-tri-*tert*-butylphenoxyl in benzene-d_6 and transferred to an nmr tube. Formation of the corresponding (^{tBu}L)FeCl(HNC$_6$H$_3$-3,5-(CF$_3$)$_2$) (**9**) (Figure S-32) was observed after 24 h in the ^{19}F NMR spectra. ^{1}H NMR spectrum revealed formation of the corresponding 2,4,6-tri-*tert*-butylphenol. Full consumption of starting complex and phenoxyl was not observed after 3 days at room temperature.

[11] Pattanayak, S.; Sinha, S. *Tet. Lett.* **2011**, *52*, 34.

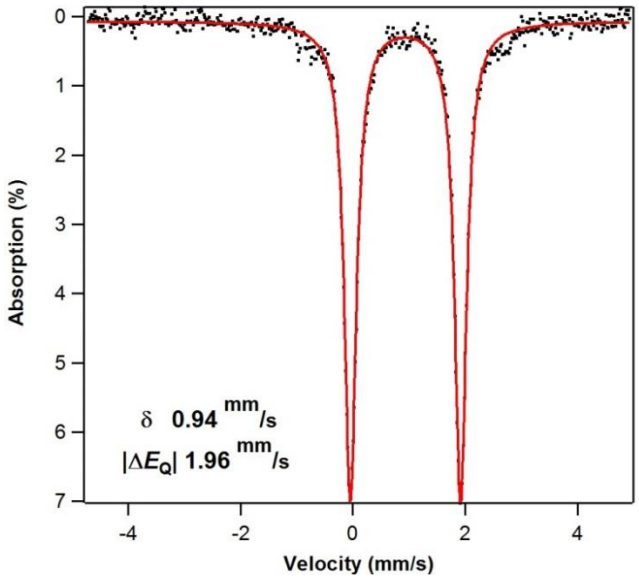

Figure S-1. Zero-field ^{57}Fe Mössbauer of [(^{tBu}L)FeCl]$_2$ (**2**) collected at 90 K. Isomer shift and quadrupole splitting are referenced to Fe foil at room temperature. Parameters calculated via single-point DFT: 50 % δ = 0.98 mm/s, ΔE_Q = –2.114 mm/s; 50 % δ = 0.98 mm/s, ΔE_Q = –2.115 mm/s.

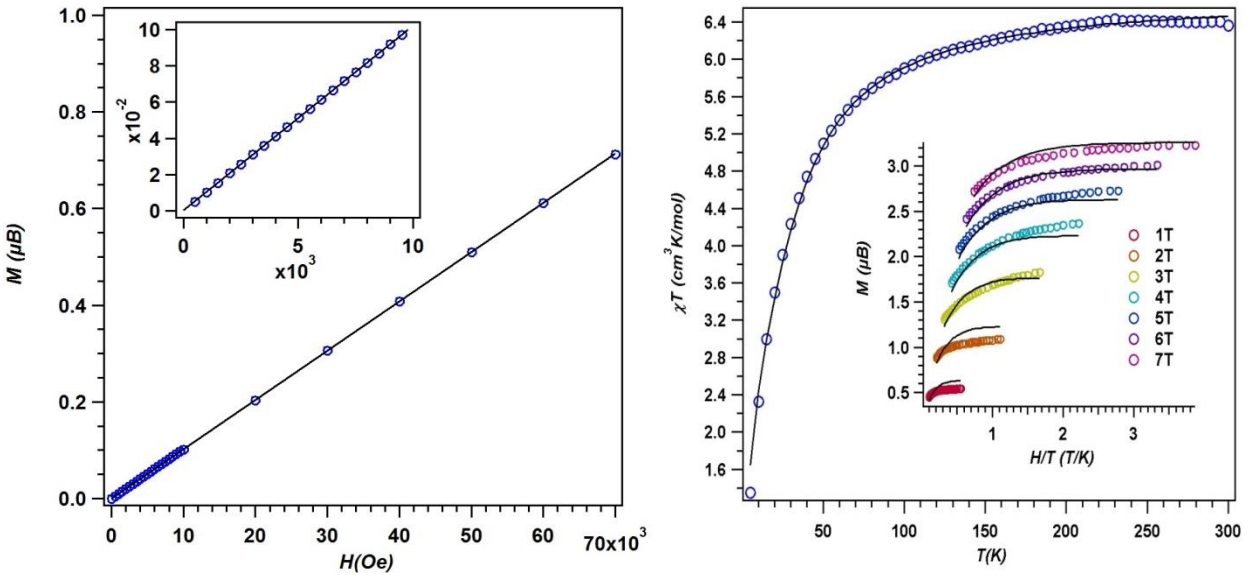

Figure S-2. Magnetization data for [(^{tBu}L)FeCl]$_2$ (**2**) **(left)** Magnetization versus field collected at 100 K – linear plot reflects the sample is free from ferromagnetic impurities; **(left inset)** *M* vs. *H* at low fields; **(right)** Variable temperature susceptibility data collected at 1.0 T, with $\chi_M T$ = 6.40 cm^{3}K/mol at 295 K; Fit parameters obtained with PHI[7]: g = 2.07, J = –1.95 cm^{-1} **(right inset)** Reduced magnetization collected at 7 fields (1-7 T) over the temperature range 1.8 – 10 K. Magnetization fit parameters obtained with PHI[7], using the coupling constant J = –1.95 cm^{-1} obtained from the fit of the $\chi_M T$ data: $g_1 = g_2$ =2.075, D_1 = 13.48 cm^{-1}, D_2 = 13.16 cm^{-1}, $|^{E1}/_{D1}|$ = 0.33, $|^{E2}/_{D2}|$ = 0.33.

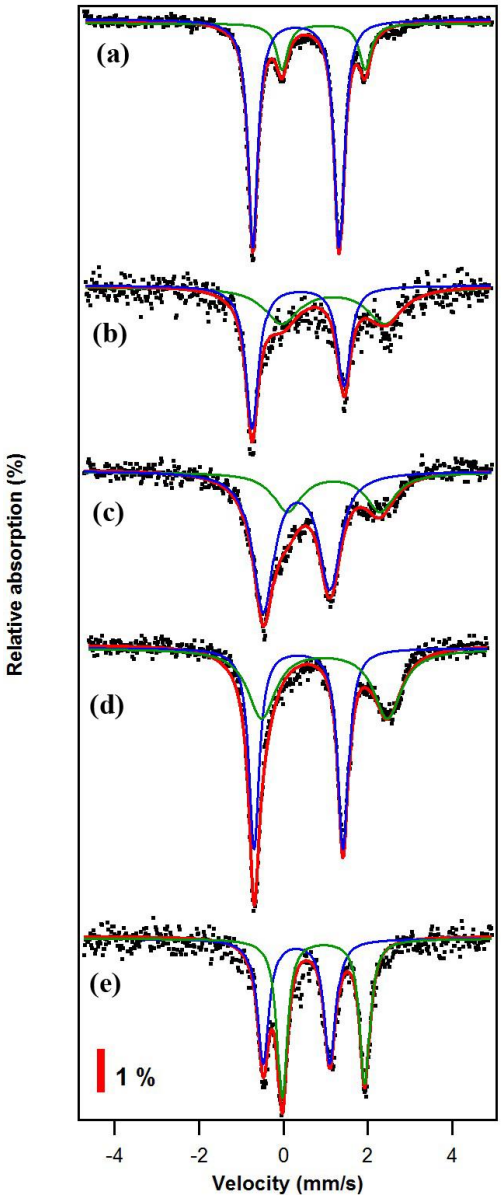

Figure S-3. Zero-field ^{57}Fe Mössbauer collected at 90 K for the reactions of [(^{tBu}L)FeCl]$_2$ (**2**) with aryl azides in benzene, for 5 min at room temperature. **(a)** 4-*tert*-butylpehnyl azide: 83 % δ = 0.30 mm/s, $|\Delta E_Q|$ = 2.04 mm/s; 17 % δ = 0.95 mm/s, $|\Delta E_Q|$ = 1.97 mm/s **(b)** 4-methoxyphenyl azide: 73 % δ = 0.34 mm/s, $|\Delta E_Q|$ = 2.18 mm/s; 27 % δ = 1.00 mm/s, $|\Delta E_Q|$ = 2.81 mm/s **(c)** 4-nitrophenyl azide: 75 % δ = 0.30 mm/s, $|\Delta E_Q|$ = 1.58 mm/s; 25 % δ = 1.15 mm/s, $|\Delta E_Q|$ = 2.34 mm/s **(d)** 2,6-diisopropylphenyl azide: 74 % δ = 0.36 mm/s, $|\Delta E_Q|$ = 2.11 mm/s; 26 % δ = 0.97 mm/s, $|\Delta E_Q|$ = 2.97 mm/s. Isomer shift and quadrupole splitting are referenced to Fe foil at room temperature. **(e)** 3,5-bis(trifluoromethyl)phenyl azide: 45 % δ = 0.32 mm/s, $|\Delta E_Q|$ = 1.57 mm/s; 55 % δ = 0.95 mm/s, $|\Delta E_Q|$ = 1.95 mm/s.

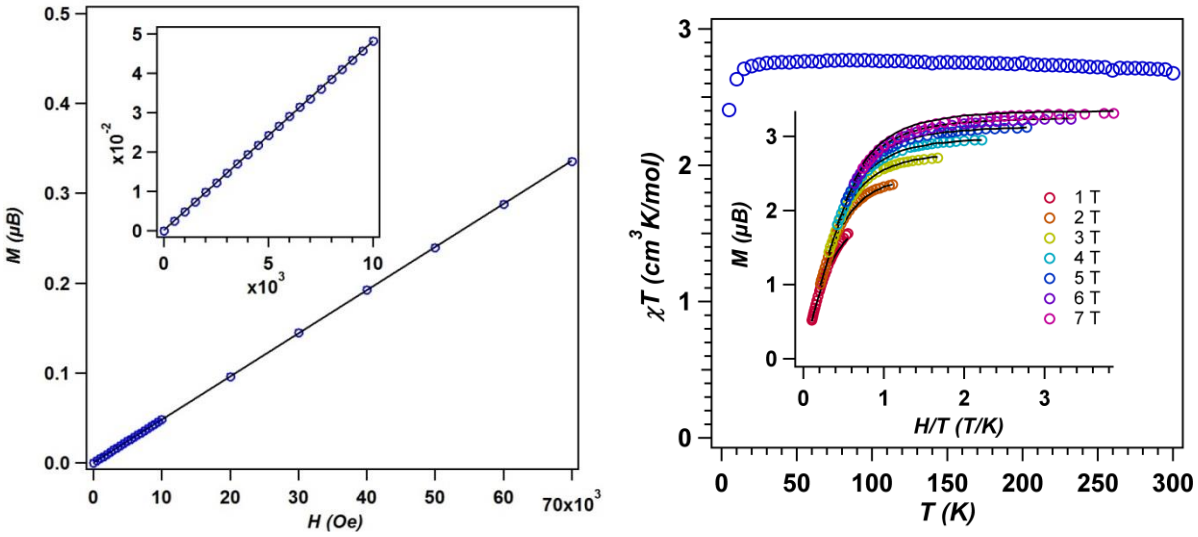

Figure S-4. Magnetization data for (^{tBu}L)FeCl($^{\bullet}$NC$_6$H$_3$-2,6-^{i}Pr$_2$) (**3**) **(left)** Magnetization versus field collected at 100 K – linear plot reflects the sample is free from ferromagnetic impurities; **(left inset)** *M* vs. *H* at low fields; **(right)** Reduced magnetization collected at 7 fields (1-7 T) over the temperature range 1.8 – 10 K. Variable temperature susceptibility data collected at 1.0 T, with $\chi_M T$ = 2.76 cm^{3}K/mol at 295 K; **(right inset)** Magnetization fit parameters obtained with PHI[7]: g = 1.95, D = 2.91 cm^{-1}, $|E/D|$ = 0.21.

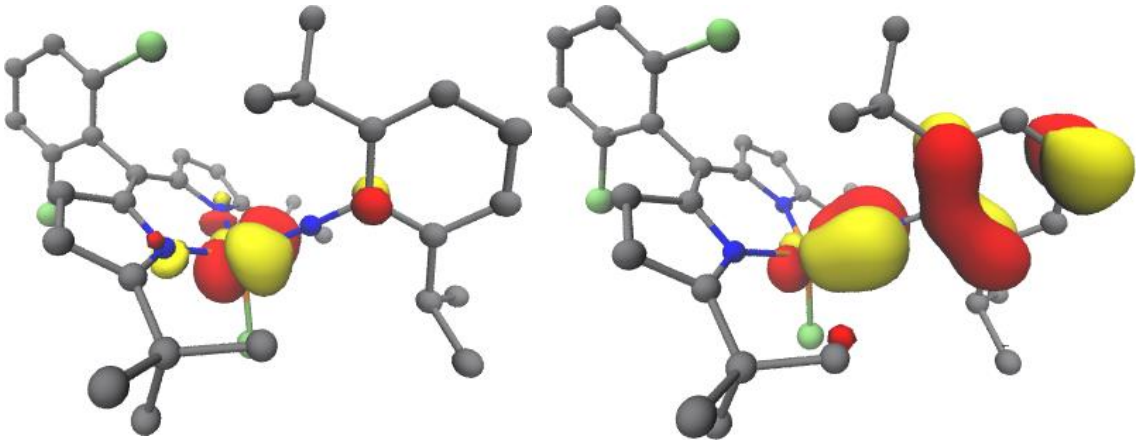

Figure S-5. Unrestricted corresponding orbitals for the spin-coupled pair (172α, 172β) derived from the BS(5,1) solution for (^{tBu}L)FeCl($^{\bullet}$NC$_6$H$_3$-2,6-^{i}Pr$_2$) (**3**).

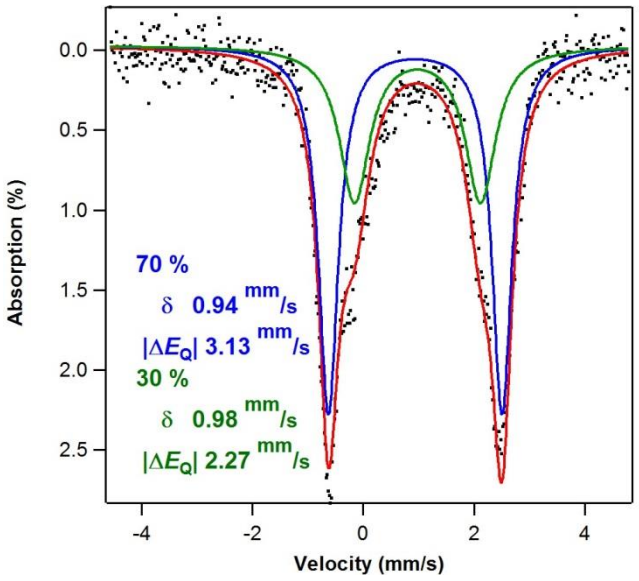

Figure S-6. Zero-field ^{57}Fe Mössbauer of (^{tBu}L)FeCl($H_2N(C_6H_3$-2-^{i}Pr-6-$C(CH_2)(Me)$)) (**4**) collected at 90 K. Isomer shift and quadrupole splitting are referenced to Fe foil at room temperature. Parameters calculated via single-point DFT: δ = 0.96 mm/s, ΔE_Q = 3.08 mm/s.

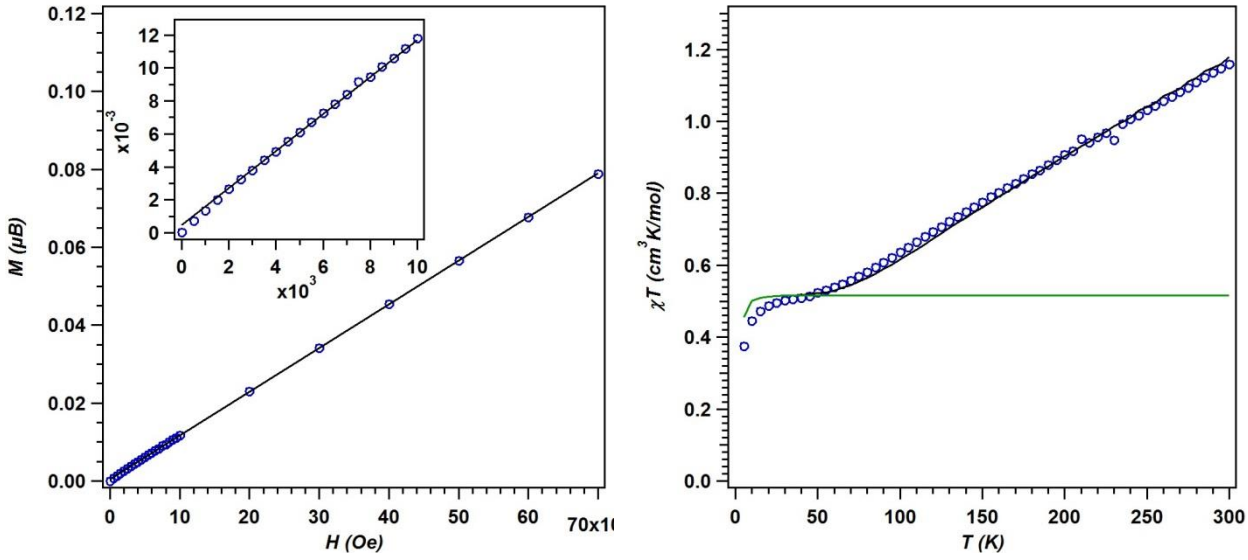

Figure S-7. Magnetization data for $[(^{tBu}L)FeCl]_2(\mu\text{-}NC_6H_3\text{-}3,5\text{-}(CF_3)_2)$ (**6**) **(left)** Magnetization versus field collected at 100 K – linear plot reflects the sample is free from ferromagnetic impurities; **(left inset)** *M* vs. *H* at low fields; **(right)** Variable temperature susceptibility data collected at 1.0 T. Fit parameters obtained with PHI[7]: g = 1.95, J = –108.7 cm^{-1}, 11.8 % impurity of a high-spin iron(III) (green trace)**.**

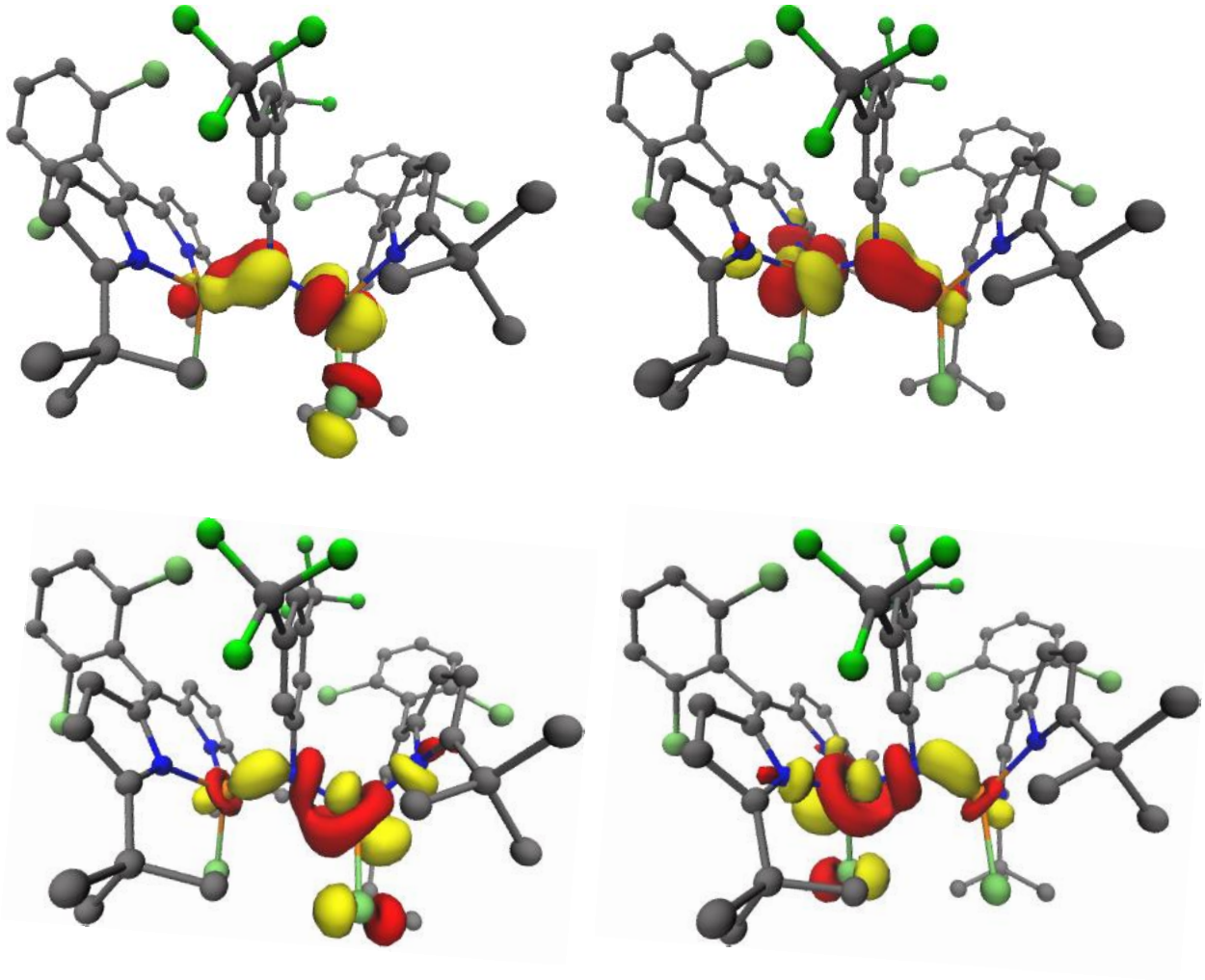

Figure S-8. Unrestricted corresponding orbitals for the spin-coupled pairs for [(^{tBu}L)FeCl]$_2$(μ-NC$_6$H$_3$-3,5-(CF$_3$)$_2$) (**6**) **(top)** (305α, 305β) and **(bottom)** (306α, 306β) derived from the BS(5,5) solution.

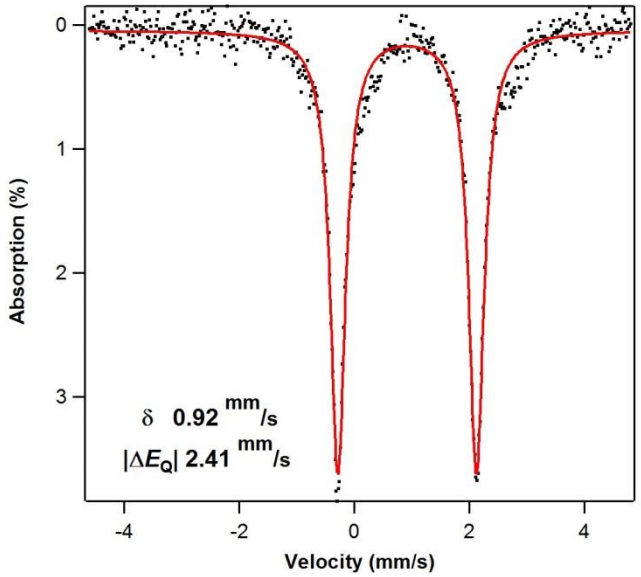

Figure S-9. Zero-field ^{57}Fe Mössbauer of (^{tBu}L)FeCl($H_2NC_6H_3$-3,5-$(CF_3)_2$) (**7**) collected at 90 K. Isomer shift and quadrupole splitting are referenced to Fe foil at room temperature. Parameters calculated via single-point DFT: δ = 0.96 mm/s, ΔE_Q = +2.28 mm/s.

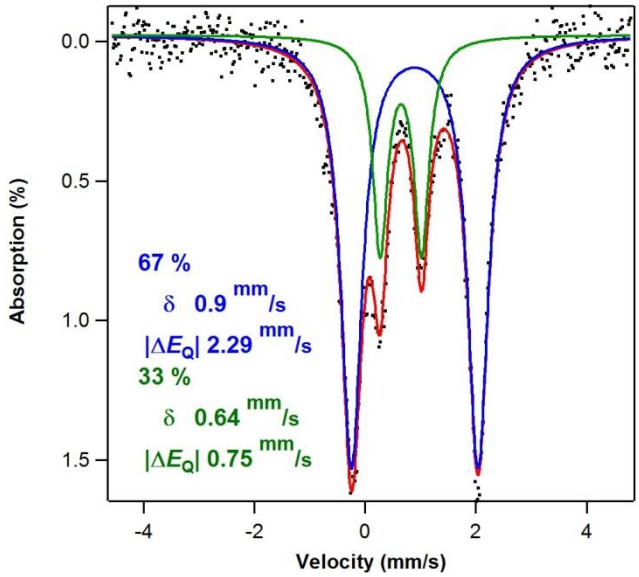

Figure S-10. Zero-field ^{57}Fe Mössbauer of [(^{tBu}L)Fe(NHC$_6$H$_3$-3,5-(CF$_3$)$_2$)]$_2$ (**8**) collected at 90 K. Isomer shift and quadrupole splitting are referenced to Fe foil at room temperature.

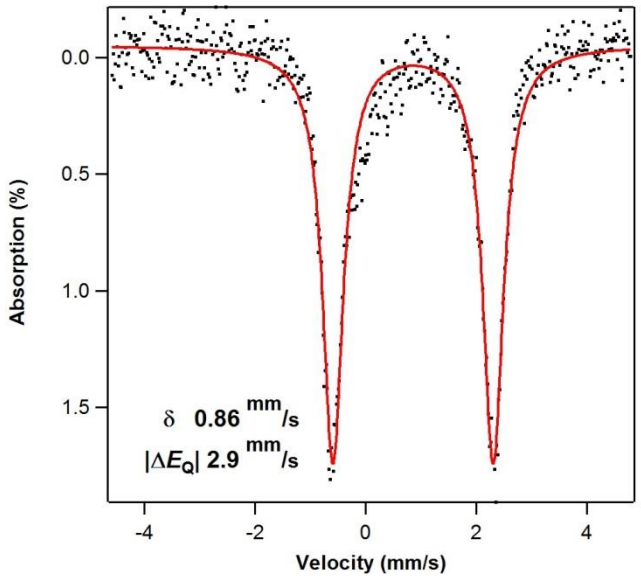

Figure S-11. Zero-field ^{57}Fe Mössbauer of (^{tBu}L)Fe(NHC$_6$H$_3$-3,5-(CF$_3$)$_2$)(py) collected at 90 K. Sample was prepared by addition of pyridine to (**8**). Isomer shift and quadrupole splitting are referenced to Fe foil at room temperature.

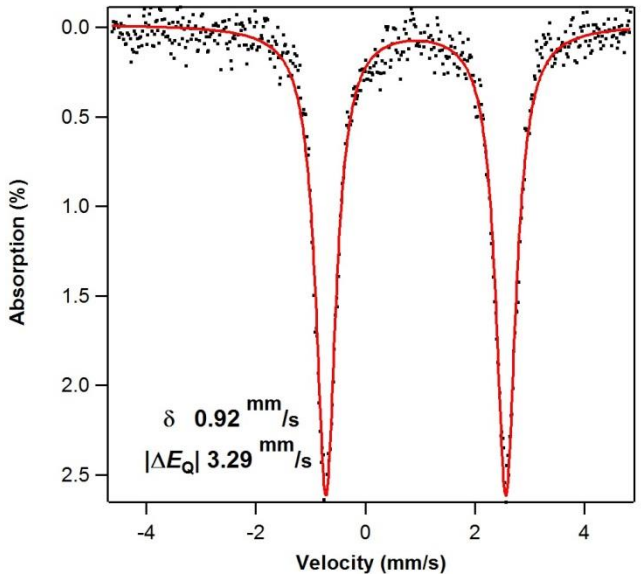

Figure S-12. Zero-field ^{57}Fe Mössbauer of [(^{tBu}L)FeCl(NHC$_6$H$_3$-3,5-(CF$_3$)$_2$)][^{n}Bu$_4$N] (**12**) collected at 90 K. Isomer shift and quadrupole splitting are referenced to Fe foil at room temperature.

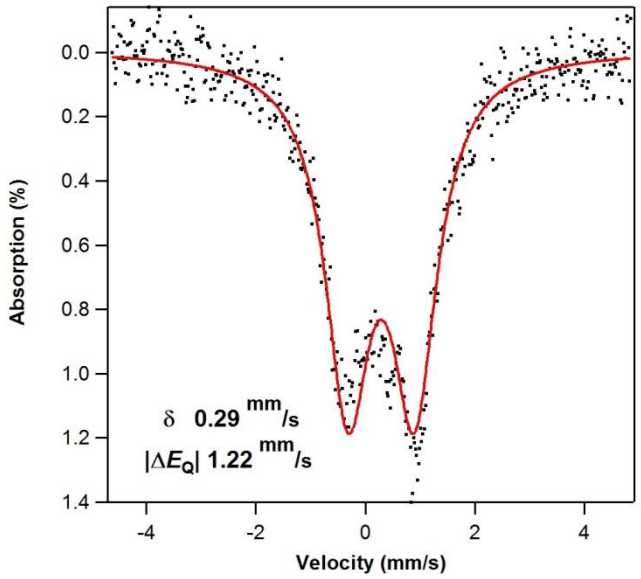

Figure S-13. Zero-field ^{57}Fe Mössbauer of (^{tBu}L)FeCl(NHC$_6$H$_3$-3,5-(CF$_3$)$_2$) (**9**) collected at 90 K. Isomer shift and quadrupole splitting are referenced to Fe foil at room temperature. Parameters calculated via single-point DFT: δ = 0.40 mm/s, ΔE_Q = +1.21 mm/s.

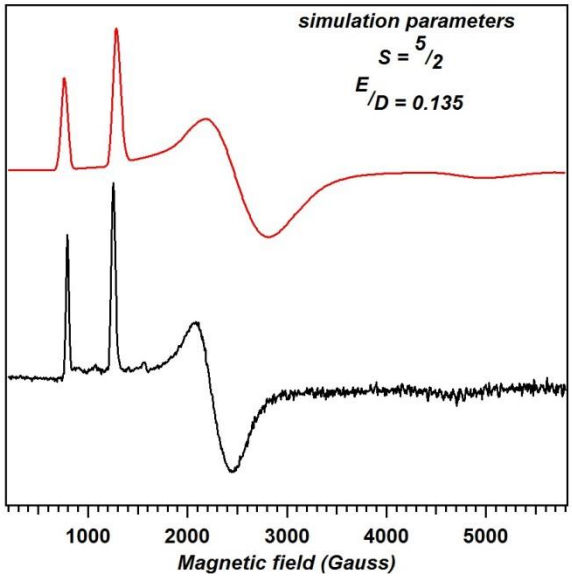

Figure S-14. Frozen solution EPR spectrum of (^{tBu}L)FeCl(NHC$_6$H$_3$-3,5-(CF$_3$)$_2$) (**9**) collected at 77 K in toluene (black). Red line represents a simulation of the data using the program VisualRhombo[6].

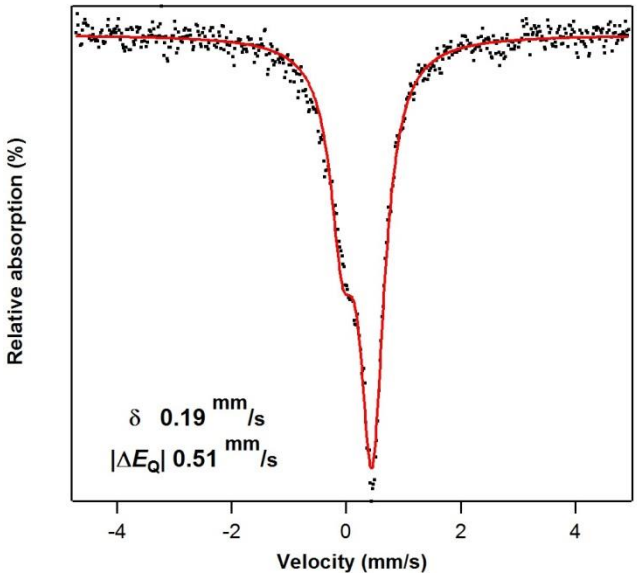

Figure S-15. Zero-field ^{57}Fe Mössbauer of (^{tBu}L)FeCl$_2$ (**10**) collected at 90 K. Isomer shift and quadrupole splitting are referenced to Fe foil at room temperature. Parameters calculated via single-point DFT: δ = 0.27 mm/s, ΔE_Q = –0.44 mm/s.

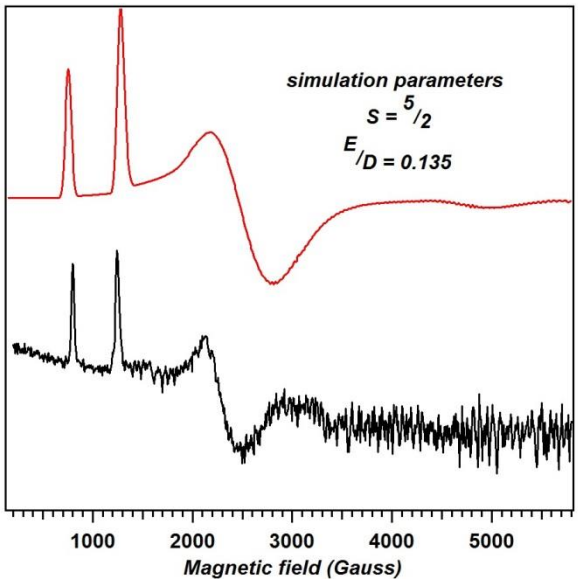

Figure S-16. Frozen solution EPR spectrum of (^{tBu}L)$FeCl_2$ (**10**) collected at 77 K in toluene (black). Red line represents a simulation of the data using the program VisualRhombo[6].

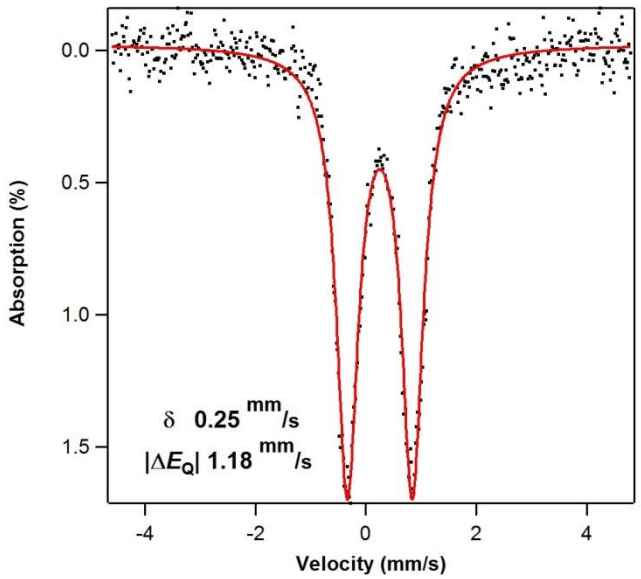

Figure S-17. Zero-field ^{57}Fe Mössbauer of (^{tBu}L)Fe(NHC$_6$H$_3$-3,5-(CF$_3$)$_2$)$_2$ (**11**) collected at 90 K. Isomer shift and quadrupole splitting are referenced to Fe foil at room temperature. Parameters calculated via single-point DFT: δ = 0.30 mm/s, ΔE_Q = –1.18 mm/s.

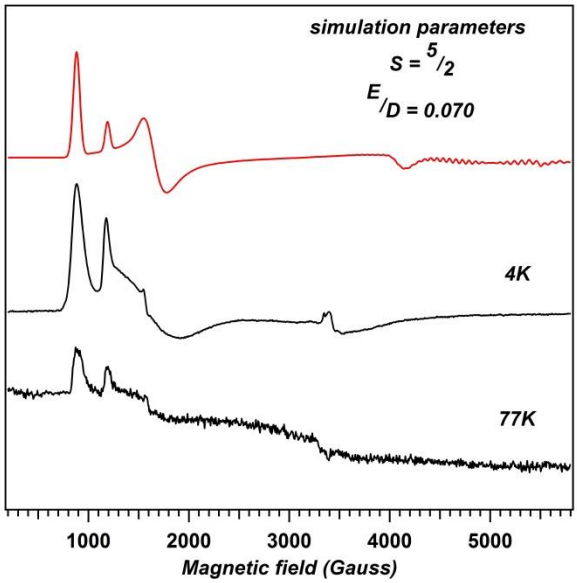

Figure S-18. Frozen solution EPR spectrum of (^{tBu}L)Fe(NHC$_6$H$_3$-3,5-(CF$_3$)$_2$)$_2$ (**11**) collected at 4 K and 77 K in toluene (black). Red line represents a simulation of the data using the program VisualRhombo[6].

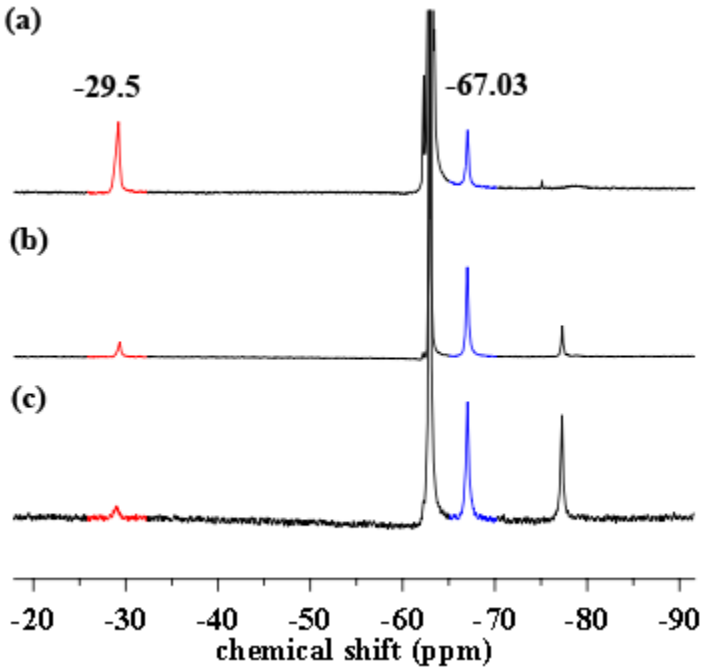

Figure S-19. ^{19}F NMR spectra of reactions of $[(^{tBu}L)FeCl]_2$ (**2**) with 3,5-bis(trifluoromethyl)phenyl azide collected immediately upon mixing the two solutions: (a) 20 equiv. of azide; (b) 1 equiv. of azide; (c) 2 equiv. of azide (relative to $[(^{tBu}L)FeCl]_2$). Proposed observed species (δ in ppm): red (δ –29.5) – $(^{tBu}L)FeCl(^{\bullet}NC_6H_3\text{-}3,5\text{-}(CF_3)_2)$; blue (δ –67.03) $[(^{tBu}L)FeCl]_2(\mu\text{-}NC_6H_3\text{-}3,5\text{-}(CF_3)_2)$; large black signal at –62.97 ppm corresponds to 3,5-bis(trifluoromethyl)phenyl azide.

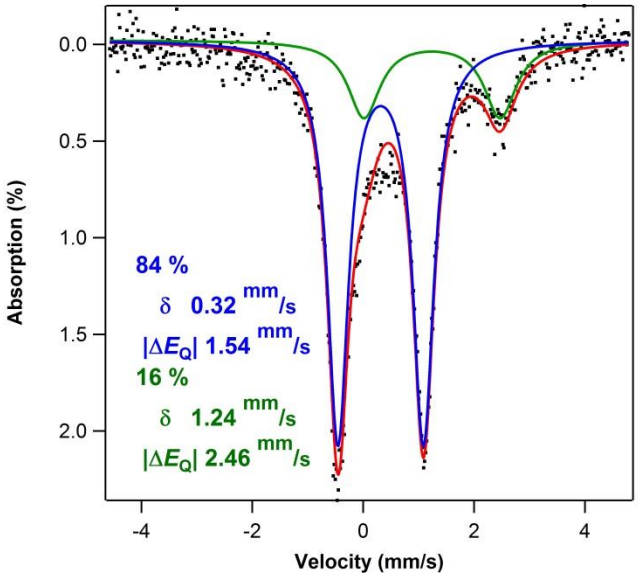

Figure S-20. Zero-field ^{57}Fe Mössbauer of the reaction mixture between **2** and 20 equiv. of 3,5-bis(trifluoromethyl)phenyl azide. Spectrum was collected at 90 K. Isomer shift and quadrupole splitting are referenced to Fe foil at room temperature.

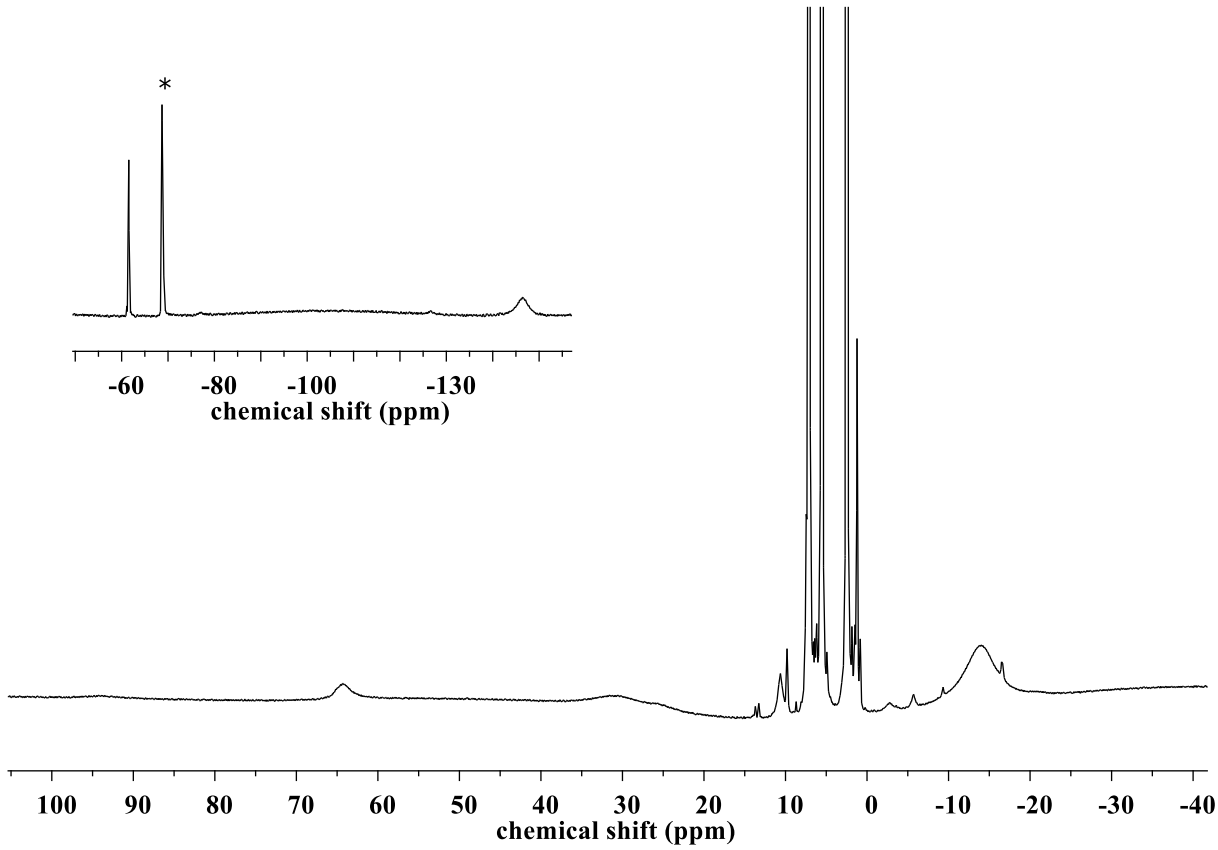

Figure S-21. ^{1}H NMR spectrum for the reaction of [(^{tBu}L)FeCl]$_2$(μ-NC$_6$H$_3$-3,5-(CF$_3$)$_2$) (**6**) with 1,4-cyclohexadiene reveals formation of (^{tBu}L)FeCl(H$_2$NC$_6$H$_3$-3,5-(CF$_3$)$_2$) (**7**); (**inset**) ^{19}F NMR spectrum displays resonances corresponding to (^{tBu}L)FeCl(H$_2$NC$_6$H$_3$-3,5-(CF$_3$)$_2$) (**7**) (*), as well as (^{tBu}L)FeCl(HNC$_6$H$_3$-3,5-(CF$_3$)$_2$) (**9**) (signal at -148.1 ppm).

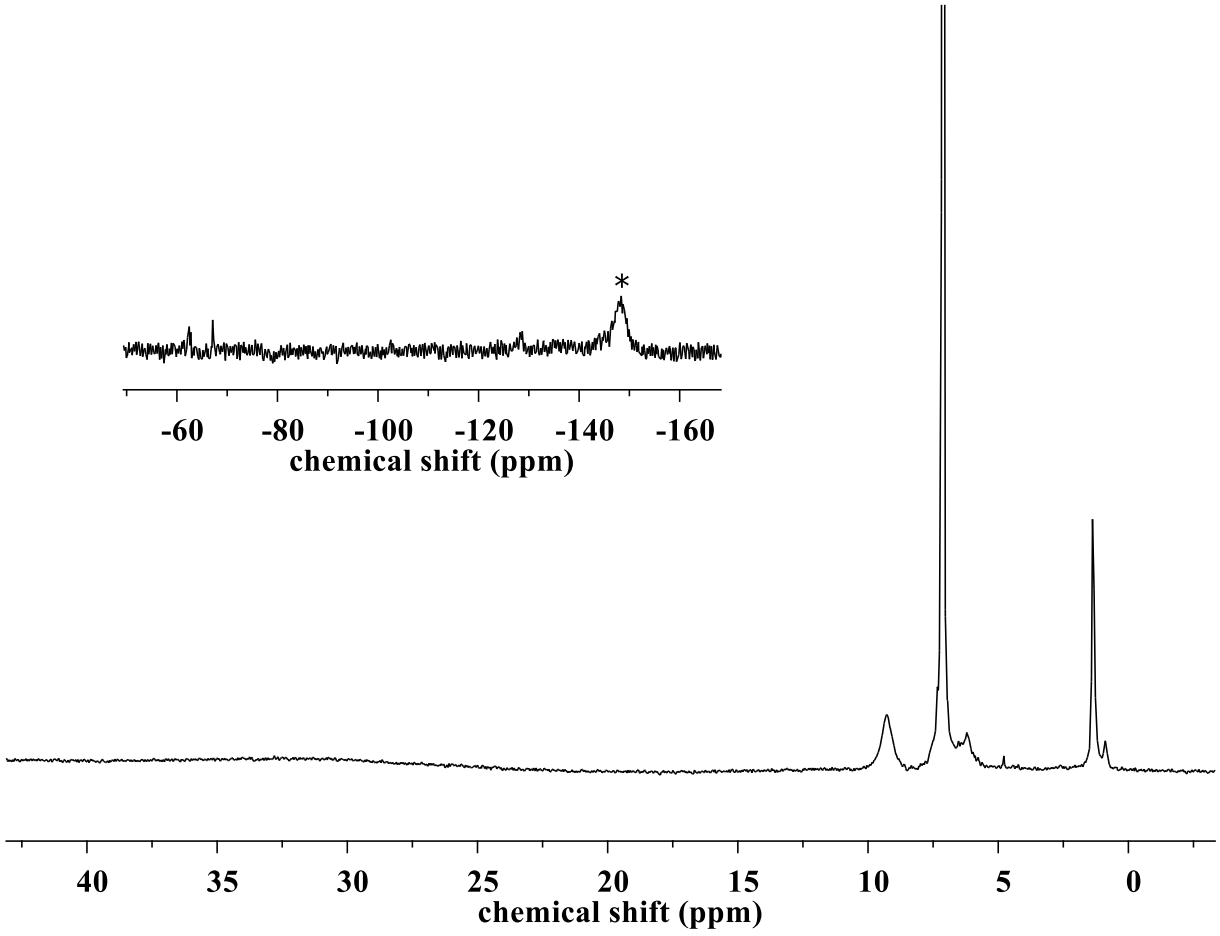

Figure S-22. ^{1}H NMR spectrum for the reaction of [(^{tBu}L)FeCl]$_2$(μ-NC$_6$H$_3$-3,5-(CF$_3$)$_2$) (**6**) with 2,4,6-tri-*tert*-butylphenol reveals formation of (^{tBu}L)FeCl(OAr) as confirmed via direct synthesis from [(^{tBu}L)FeCl]$_2$ and 2,4,6-tri-*tert*-butylphenoxyl radical; (**inset**) ^{19}F NMR spectrum displays resonances corresponding to (^{tBu}L)FeCl(HNC$_6$H$_3$-3,5-(CF$_3$)$_2$) (**9**) (*).

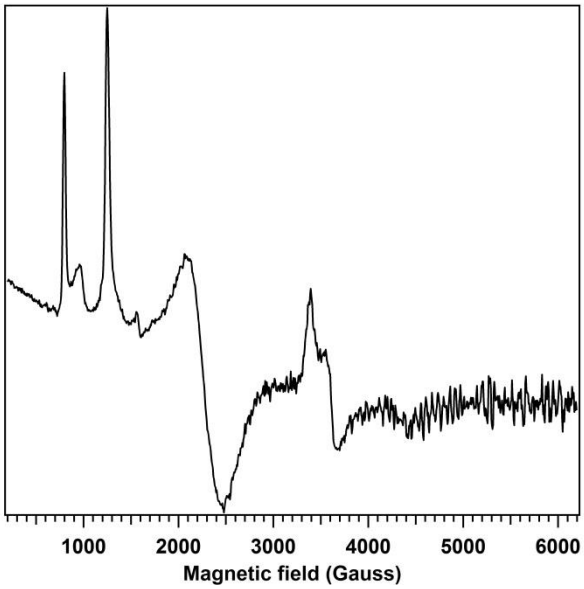

Figure S-23. Frozen solution EPR spectrum of a solution of $[(^{tBu}L)FeCl]_2(\mu\text{-}NC_6H_3\text{-}3,5\text{-}(CF_3)_2)$ (**6**) in benzene-d_6 after standing at room temperature for 30 min**.** Spectrum collected at 77 K in toluene g_{eff} = 1.99, 1.87, 1.53 and g_{eff} = 8.45, 5.39, 2.99. A new identifiable g value at 7.06 is observed after 30 min, however, corresponding g values cannot be easily assigned from these spectra.

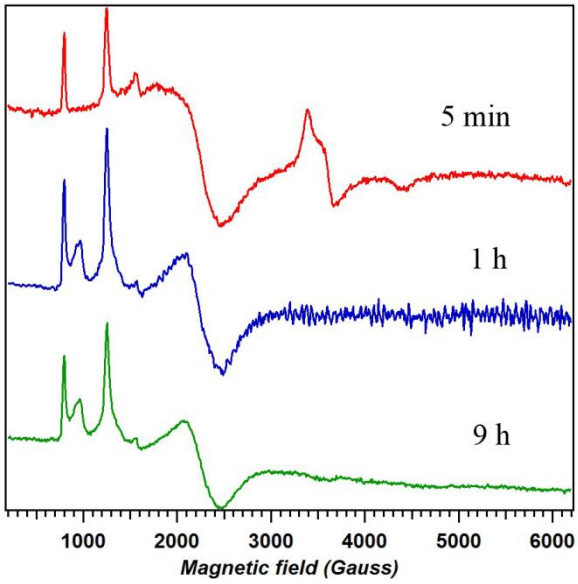

Figure S-24. Frozen solution EPR spectra for the reaction of $[(^{tBu}L)FeCl]_2$ (**2**) with 3,5-bis(trifluoromethyl)phenyl azide collected at 77 K in toluene at different time points. Spectrum after 5 min: g_{eff} = 1.99, 1.87, 1.53 and g_{eff} = 8.45, 5.39, 2.99. A new identifiable g value at 7.06 is observed after 1 hour, however, corresponding g values cannot be easily assigned from these spectra.

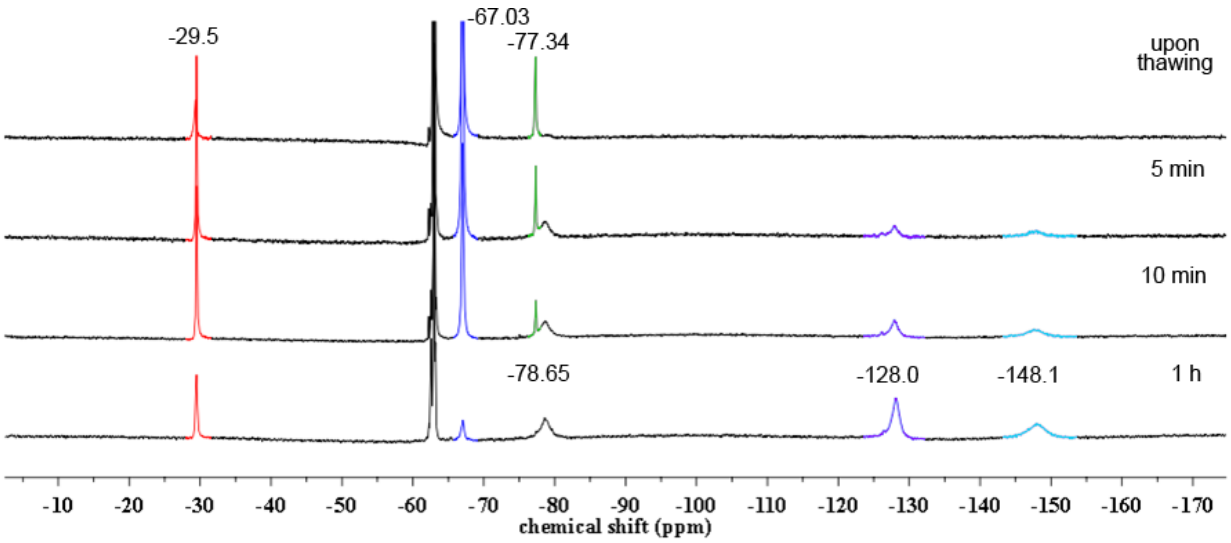

Figure S-25. ^{19}F NMR time course for the reaction of [(^{tBu}L)FeCl]$_2$ (**2**) with 3,5-bis(trifluoromethyl)phenyl azide in benzene-d_6. Unlabeled peak at –62.97 ppm corresponds to 3,5-bis(trifluoromethyl)phenyl azide.

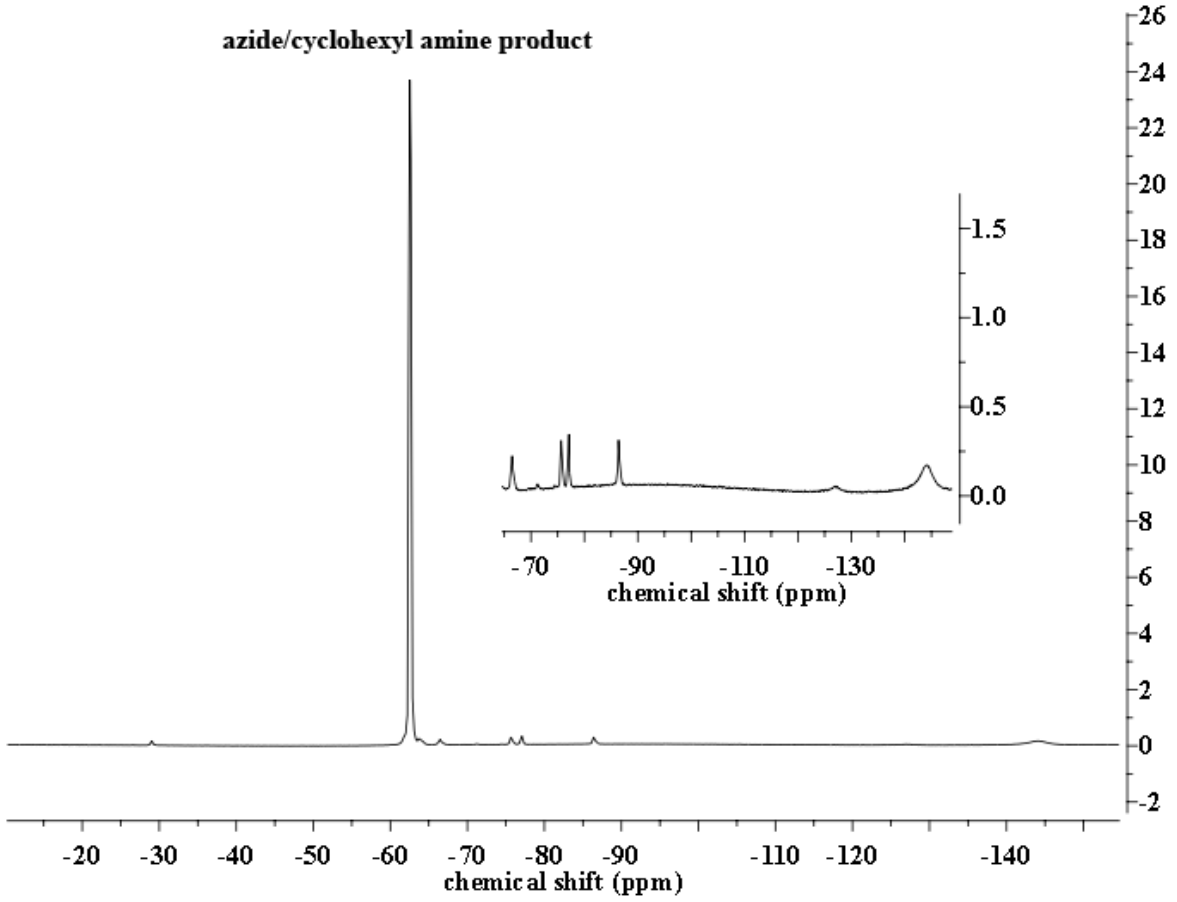

Figure S-26. ^{19}F NMR spectrum for the catalytic reaction of $[(^{tBu}L)FeCl]_2$ (**2**) with 3,5-bis(trifluoromethyl)phenyl azide in cyclohexene after 10 min reveals the relative amounts of organic products and iron-containing species (**inset**) formed during the reaction.

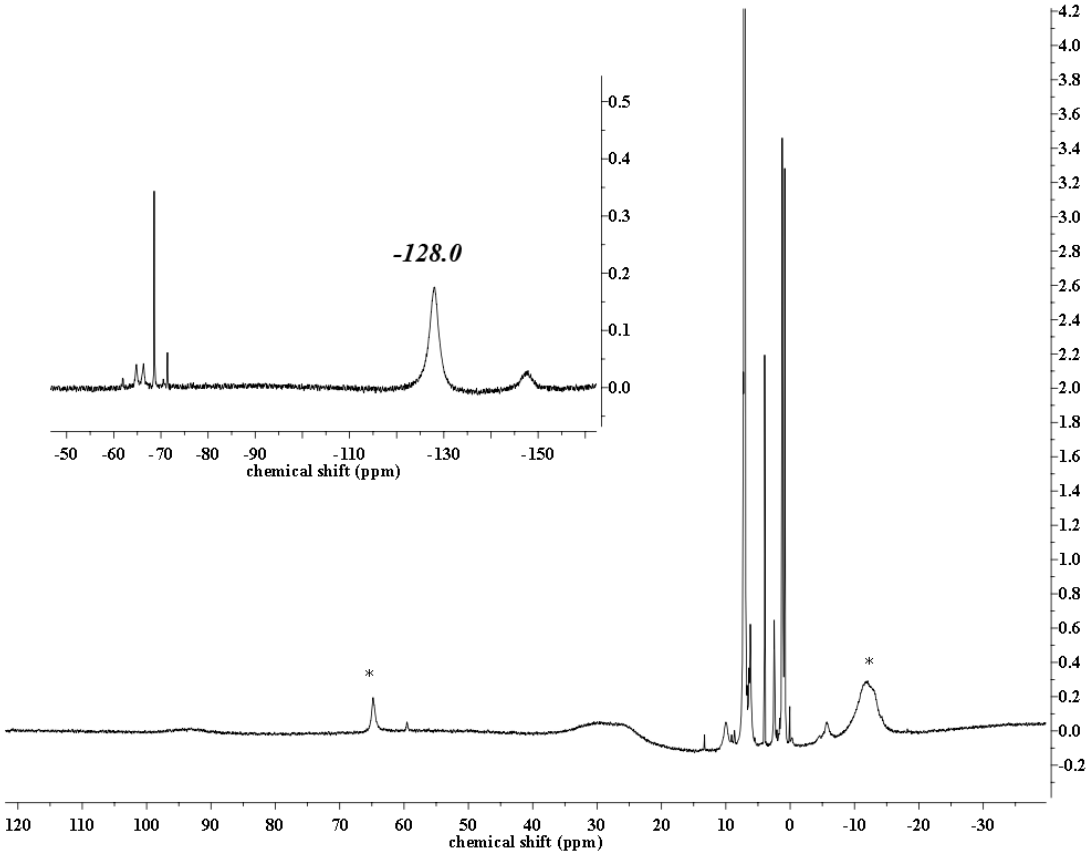

Figure S-27. Synthesis of (^{tBu}L)Fe(HNC$_6$H$_3$-3,5-(CF$_3$)$_2$)$_2$ (**11**) via ligand exchange. ^{1}H NMR reveals formation of [(^{tBu}L)FeCl]$_2$ (**2**) (peaks marked as *); **(inset)** ^{19}F NMR displays resonance at –128.0 ppm, indicating formation of ^{tBu}LFe(HNC$_6$H$_3$-3,5-(CF$_3$)$_2$)$_2$ (**11**).

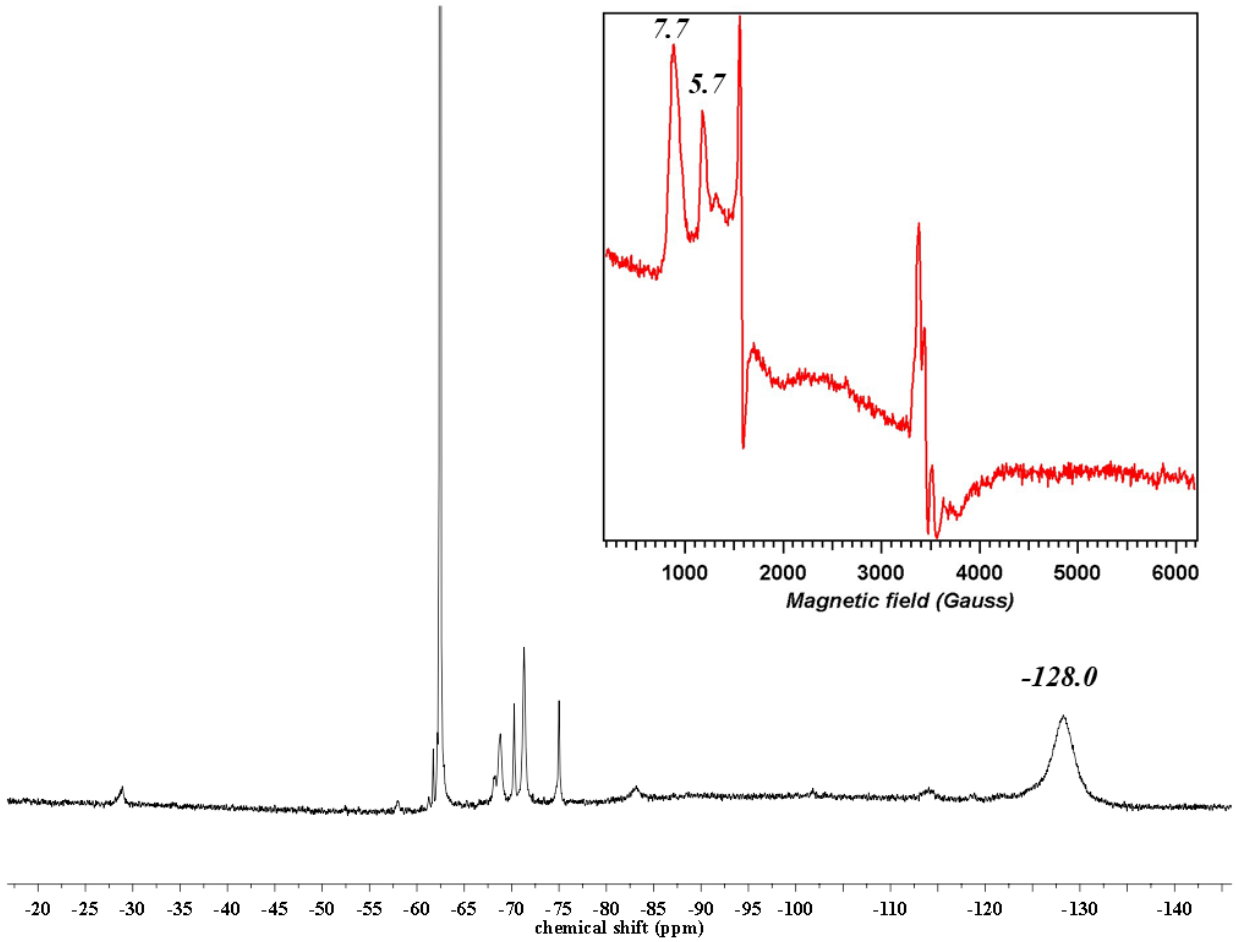

Figure S-28. Synthesis of (^{tBu}L)Fe(HNC$_6$H$_3$-3,5-(CF$_3$)$_2$)$_2$ (**11**) from [(^{tBu}L)Fe(HNC$_6$H$_3$-3,5-(CF$_3$)$_2$)]$_2$ (**8**) and 3,5-bis(trifluoromethyl)phenyl azide. ^{19}F NMR reveals formation of (^{tBu}L)Fe(HNC$_6$H$_3$-3,5-(CF$_3$)$_2$)$_2$ (**11**) (peak at –128.0 ppm); **(inset)** Frozen solution EPR (toluene, 77 K) spectrum of the reaction mixture after 30 min reveals signal corresponding to (^{tBu}L)Fe(HNC$_6$H$_3$-3,5-(CF$_3$)$_2$)$_2$ (**11**): 7.7, 5.7.

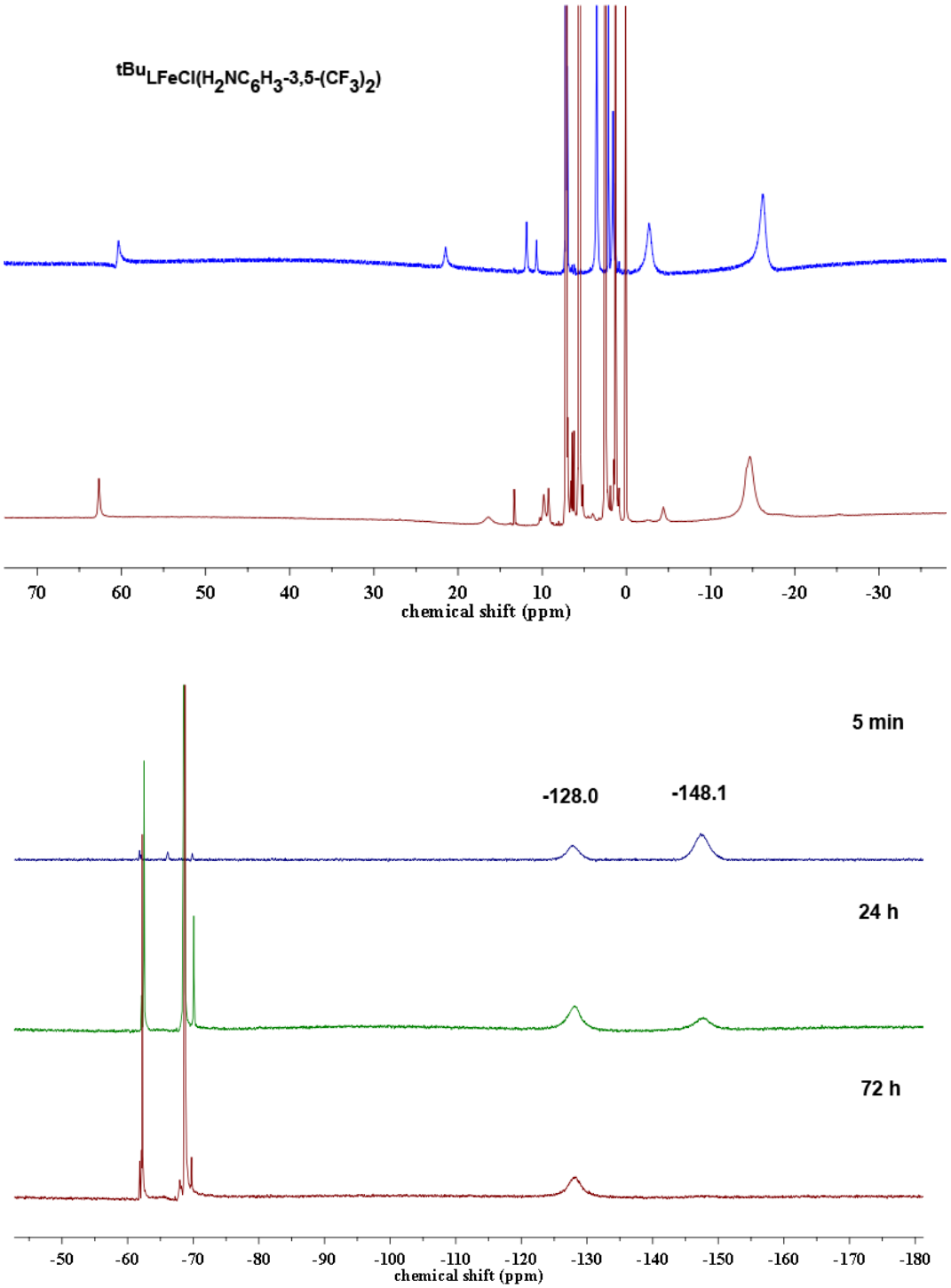

Figure S-29. Reaction of (^{tBu}L)FeCl(HNC$_6$H$_3$-3,5-(CF$_3$)$_2$) (**9**) and (^{tBu}L)Fe(HNC$_6$H$_3$-3,5-(CF$_3$)$_2$)$_2$ (**11**) with 1,4-cyclohexadiene at 65 °C; (**top**) ^{1}H NMR spectrum of (^{tBu}L)FeCl(H$_2$NC$_6$H$_3$-3,5-(CF$_3$)$_2$) (**7**) (blue) overlaid with spectrum of the reaction mixture acquired after 72 hours (red); (**bottom**) ^{19}F NMR time course of the reaction.

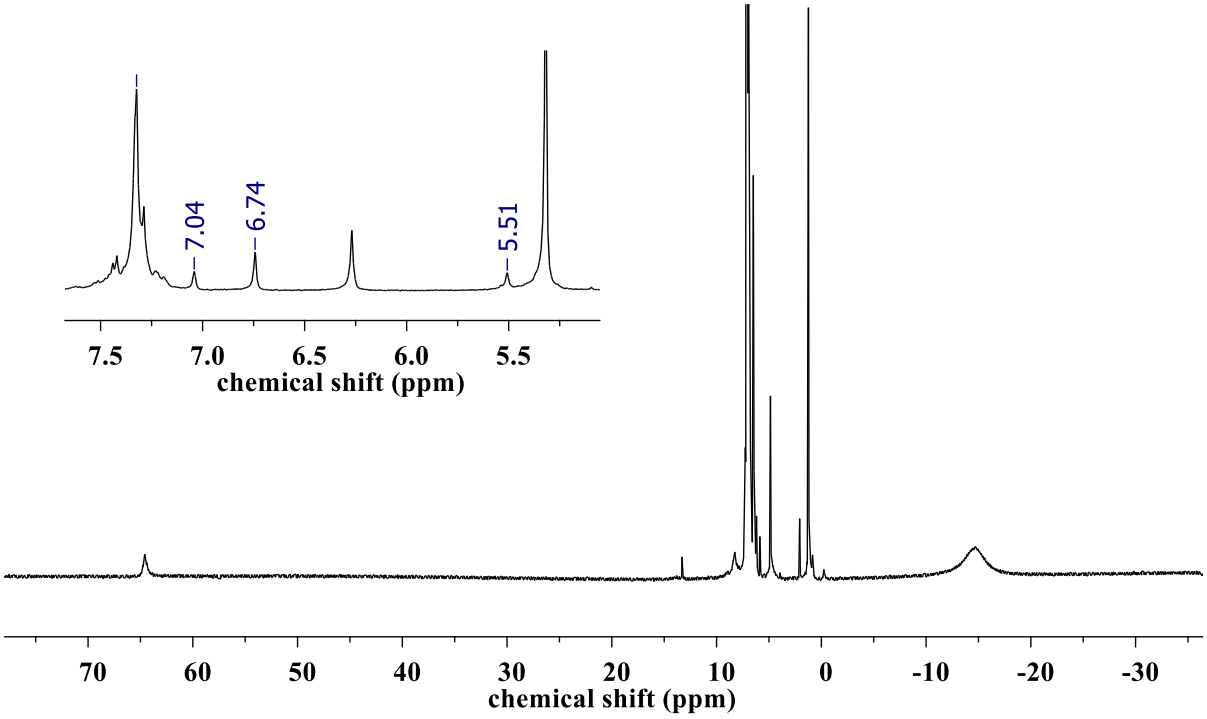

Figure S-30. Reaction of (^{tBu}L)FeCl(HNC$_6$H$_3$-3,5-(CF$_3$)$_2$) (**9**) with triphenylmethyl radical: ^{1}H NMR spectrum reveals formation of [(^{tBu}L)FeCl]$_2$ (**2**); (**inset**) ^{1}H NMR spectrum after work-up reveals formation of 3,5-bis(trifluoromethyl)-*N*-tritylaniline.

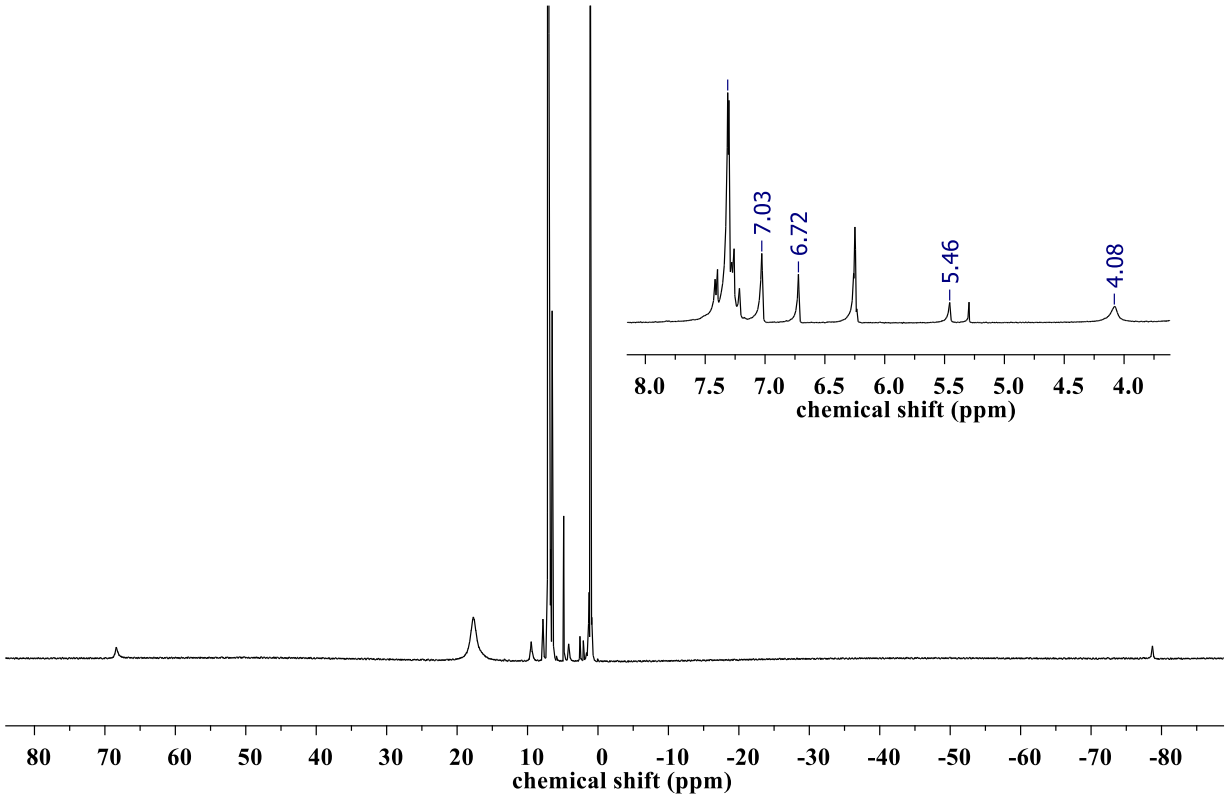

Figure S-31. Reaction of (^{tBu}L)Fe(HNC$_6$H$_3$-3,5-(CF$_3$)$_2$)$_2$ (**11**) with trityl radical: ^{1}H NMR spectrum reveals formation of [(^{tBu}L)Fe(HNC$_6$H$_3$-3,5-(CF$_3$)$_2$)]$_2$ (**8**); (**inset**) ^{1}H NMR spectrum after work-up reveals formation of both 3,5-bis(trifluoromethyl)-*N*-tritylaniline and 3,5-bis(trifluoromethyl)aniline.

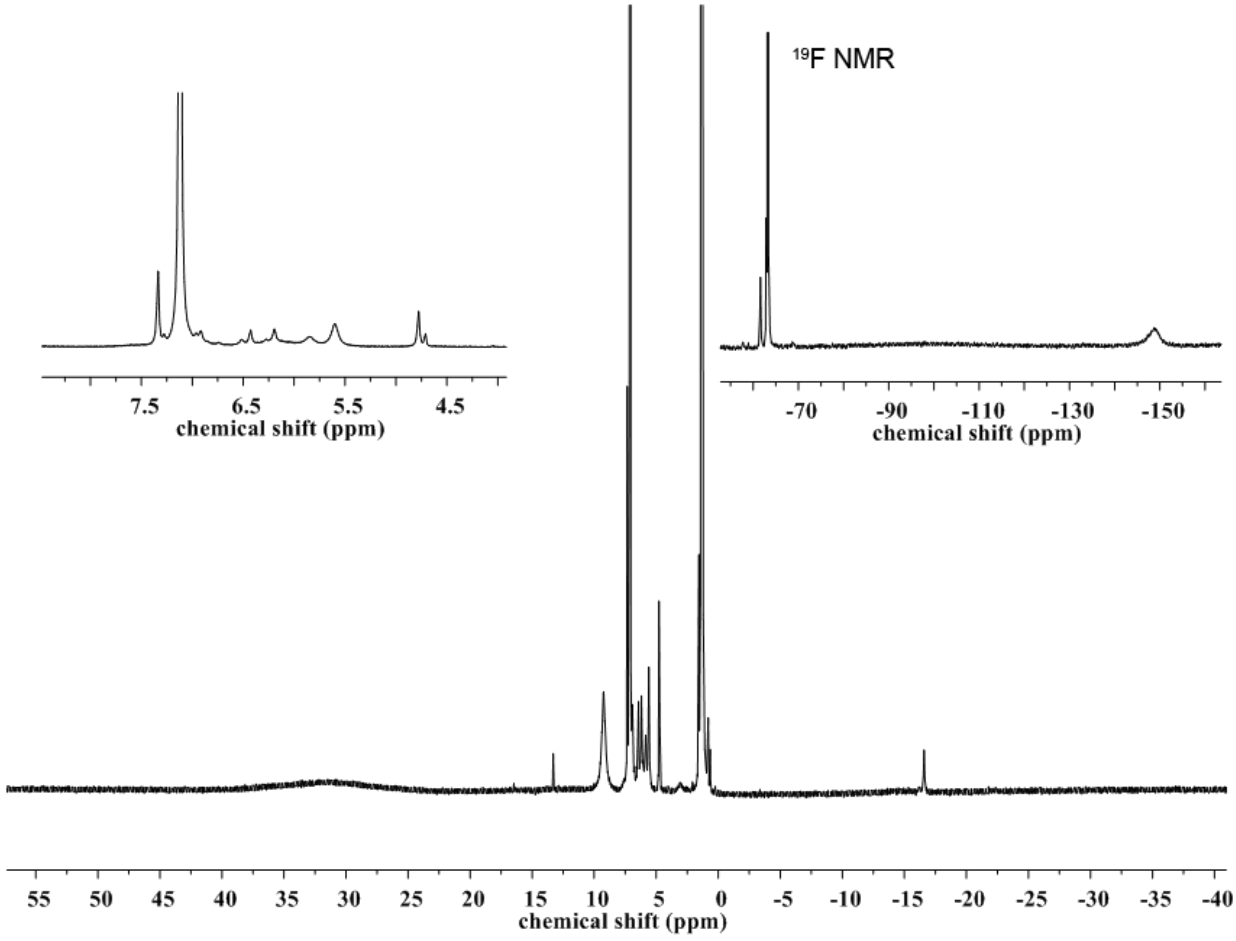

Figure S-32. Reaction of (^{tBu}L)FeCl($H_2NC_6H_3$-3,5-$(CF_3)_2$) (**7**) with 2,4,6-tri-*tert*-butylphenoxyl radical: ^{1}H NMR spectrum after 24 h; (**left inset**) ^{1}H NMR spectrum reveals formation of the corresponding 2,4,6-tri-*tert*-butylphenol; (**right inset**) ^{19}F NMR spectrum reveals formation of (^{tBu}L)FeCl(HNC_6H_3-3,5-$(CF_3)_2$) (**9**).

X-Ray Diffraction Techniques. All structures were collected on a Bruker three-circle platform goniometer equipped with an Apex II CCD and an Oxford cryostream cooling device. Radiation was from a graphite fine focus sealed tube Mo Kα (0.71073 Å) source. Crystals were mounted on a cryoloop or glass fiber pin using Paratone N oil. Structures were collected at 100 K. Data was collected as a series of φ and/or ω scans. Data was integrated using SAINT[12] and scaled with either a numerical or multi-scan absorption correction using SADABS[12]. The structures were solved by direct methods or Patterson maps using SHELXS-97[13] and refined against F^2 on all data by full matrix least squares with SHELXL-97[13]. All non-hydrogen atoms were refined anisotropically. Hydrogen atoms were placed at idealized positions and refined using a riding model. The isotropic displacement parameters of all hydrogen atoms were fixed to 1.2 times the atoms they are linked to (1.5 times for methyl groups). Further details on particular structures are noted below.

[(^{tBu}L)FeCl]$_2$ (2). The structure was solved in the monoclinic space group $P2_1/n$ with 2 molecules per unit cell.

(^{tBu}L)FeCl($^{\bullet}$NC$_6$H$_3$-2,6-^{i}Pr$_2$) (3). The structure was solved in the monoclinic space group $P2_1/c$ with 4 molecules per unit cell. A fluorobenzene solvent molecule exhibited disorder and was modeled using similarity constraints.

(^{tBu}L)FeCl(H$_2$NC$_6$H$_3$-2-^{i}Pr$_2$-6-C(CH$_2$)(CH$_3$)) (4). The structure was solved in the orthorhombic space group *Pbca* with 4 molecules per unit cell. A benzene solvent molecule exhibited disorder and was modeled using constraints.

[(^{tBu}L)FeCl]$_2$(μ-NC$_6$H$_3$-3,5-(CF$_3$)$_2$) (6). The structure was solved in the triclinic space group $P\bar{1}$ with 2 molecules per unit cell. A disordered benzene solvent molecule was modeled with similarity constraints and refined with half occupancies for the unit cell.

(^{tBu}L)FeCl(H$_2$NC$_6$H$_3$-3,5-(CF$_3$)$_2$) (7). The structure was solved in the monoclinic space group $P2_1/c$ with 4 molecules per unit cell. One of the chloride bound to the iron center was disordered and modeled with similarity constraints. A benzene solvent molecule lies on a special position and was refined with half occupancy for the asymmetric unit.

[12] *APEX2 Software Suite*; Bruker AXS: Madison, WI, 2014.
[13] Sheldrick, G. M. Acta Crystallogr., Sect. A: Found. Crystallogr. **2008**, 64, 112-122.

[(^{tBu}L)FeCl(HNC$_6$H$_3$-3,5-(CF$_3$)$_2$)]$_2$ (8). The structure was solved in the monoclinic space group *C2/c* with 8 molecules per unit cell. A disordered hexanes solvent molecule lies on a special position and was refined with half occupancies for the asymmetric unit cell and modeled using similarity constraints.

(^{tBu}L)FeCl(HNC$_6$H$_3$-3,5-(CF$_3$)$_2$) (9). The structure was solved in the triclinic space group $P\bar{1}$ with 2 molecules per unit cell. A benzene solvent molecule lies on a special position and was refined with half occupancies.

(^{tBu}L)FeCl$_2$ (10). The structure was solved in the monoclinic space group *Cc* with 4 molecules per unit cell.

(^{tBu}L)Fe(HNC$_6$H$_3$-3,5-(CF$_3$)$_2$)$_2$ (11). The structure was solved in the triclinic space group $P\bar{1}$ with 2 molecules per unit cell. Disordered trifluoromethyl groups were modeled using similarity constraints. Due to high disorder of the hexanes solvent molecule, an acceptable model could not be refined. Instead, a solvent mask was implemented in the Olex2 software which did not seriously affect the chemically significant features of the structure.

Table S-1. X-ray diffraction experimental details[a,b]

	[(^{tBu}L)FeCl]$_2$ (2)	**(^{tBu}L)FeCl($^{\cdot}$NC$_6$H$_3$-2,6-^{i}Pr$_2$) (3)**	**(^{tBu}L)FeCl(H$_2$NC$_6$H$_3$-2-^{i}Pr$_2$-6-C(CH$_2$)(CH$_3$)) (4)**	**[(^{tBu}L)FeCl]$_2$(μ-NC$_6$H$_3$-3,5-(CF$_3$)$_2$) (6)**	**[(^{tBu}L)Fe(H$_2$NC$_6$H$_3$-3,5-(CF$_3$)$_2$)]$_2$ (7)**
Moiety Formula	$C_{23}H_{25}Cl_3FeN_2$; C_6H_6	$C_{35}H_{42}Cl_3FeN_3$; 0.5× (C_6H_5F)	$C_{35}H_{42}Cl_3FeN_3$; 3×(C_3H_3)	$C_{54}H_{53}Cl_6Fe_2N_5$; 0.5×(C_6H_6)	2×($C_{31}H_{30}Cl_3F_6FeN_3$) ; 0.5×(C_6H_6)
FW	569.76	714.96	784.07	1249.46	1480.61
Crystal System	monoclinic	monoclinic	orthorhombic	triclinic	monoclinic
Space Group (Z)	$P2_1/n$ (2)	$P2_1/c$ (4)	*Pbca* (8)	$P\bar{1}$ (2)	$P2_1/c$ (4)
a (Å)	13.4486(11)	12.1706(18)	23.270(2)	12.7480(9)	13.6061(6)
b (Å)	10.8936(9)	16.847(3)	14.7919(14)	13.0508(9)	31.1222(14)
c (Å)	18.8713(16)	19.035(3)	24.359(2)	19.9343(13)	17.3548(7)
α (°)	90	90	90	96.7240(13)	90
β (°)	94.695(2)	93.660(3)	90	96.7310(13)	103.397(1)
γ (°)	90	90	90	113.9150(12)	90
Volume (Å^3)	2755.4(4)	3895.0(10)	8384.4(13)	2961.0(4)	7148.9(5)
Calc. ρ (mg/m^3)	1.373	1.219	1.242	1.400	1.376
μ (mm^{-1})	0.859	0.624	0.584	0.820	0.703
Crystal Size (mm)	0.34×0.21×0.08	0.45×0.35×0.22	1.0×0.238×0.29	0.23×0.11×0.10	0.21×0.11×0.1
Reflections	4871	6907	7388	10580	12782
Completeness (to 2θ)	99.8% 25.04°	99.1% 25.148°	99.5% 25.056°	99.0% 25.222°	98.9% 25.222 °
GOF on F^2	0.882	1.121	1.0777	1.058	1.029
R1, wR2[c] [I>2σ(I)]	0.0295, 0.0522	0.0520, 0.1765	0.0572, 0.1571	0.0614, 0.1925	0.0784, 0.2255

[a] λ = 0.71073 Å; [b] T = 100(2) K; [c] $R1 = \Sigma||F_o|-|F_c||/\Sigma|F_o|$, $wR2 = \{\Sigma[w(F_o^2-F_c^2)^2]/\Sigma[w(F_o^2)^2]\}^{1/2}$

	[(^{tBu}L)Fe(HNC$_6$H$_3$-3,5-(CF$_3$)$_2$)]$_2$ (8)	**(^{tBu}L)FeCl(HNC$_6$H$_3$-3,5-(CF$_3$)$_2$) (9)**	**(^{tBu}L)FeCl$_2$ (10)**	**(^{tBu}L)Fe(HNC$_6$H$_3$-3,5-(CF$_3$)$_2$)$_2$ (11)**
Moiety Formula	$C_{31}H_{29}Cl_2F_6FeN_3$; 0.5×(C_3H_7)	$C_{31}H_{29}Cl_3FeN_3$; C_6H_6	$C_{23}H_{25}Cl_4FeN_2$	$C_{39}H_{33}Cl_2F_{12}FeN_4$
FW	705.86	797.88	527.10	912.44
Crystal System	monoclinic	triclinic	monoclinic	triclinic
Space Group (Z)	*C2/c* (8)	$P\bar{1}$ (2)	*Cc* (4)	$P\bar{1}$ (2)
a (Å)	22.108(3)	12.267 (4)	15.064(2)	11.6153(11)
b (Å)	11.9657(17)	12.613(4)	17.537(3)	11.8003(10)
c (Å)	25.005(4)	13.807(4)	11.077(3)	16.1066(15)
α (°)	90	76.462(4)	90	73.913(2)
β (°)	90	82.700(4)	126.613(2)	88.916(2)
γ (°)	90	71.185(4)	90	85.031(2)
Volume (Å^3)	6614.8(17)	1962.8(11)	2348.9(8)	2113.2(3)
Calc. ρ (mg/m^3)	1.418	1.350	1.490	1.434
μ (mm^{-1})	0.678	0.646	1.111	0.569
Crystal Size (mm)	0.27×0.26×0.16	0.24×0.16×0.12	0.32×0.12×0.11	0.24×0.22×0.11
Reflections	5802	6590	4189	7449
Completeness (to 2θ)	97.9% 24.985°	95.2% 24.995°	99% 25.204°	98.6% 25.129°
GOF on F^2	0.954	1.038	1.023	1.036
R1, wR2^c [I>2σ(I)]	0.0597, 0.1605	0.0923, 0.3026	0.0271, 0.0478	0.0587, 0.1322

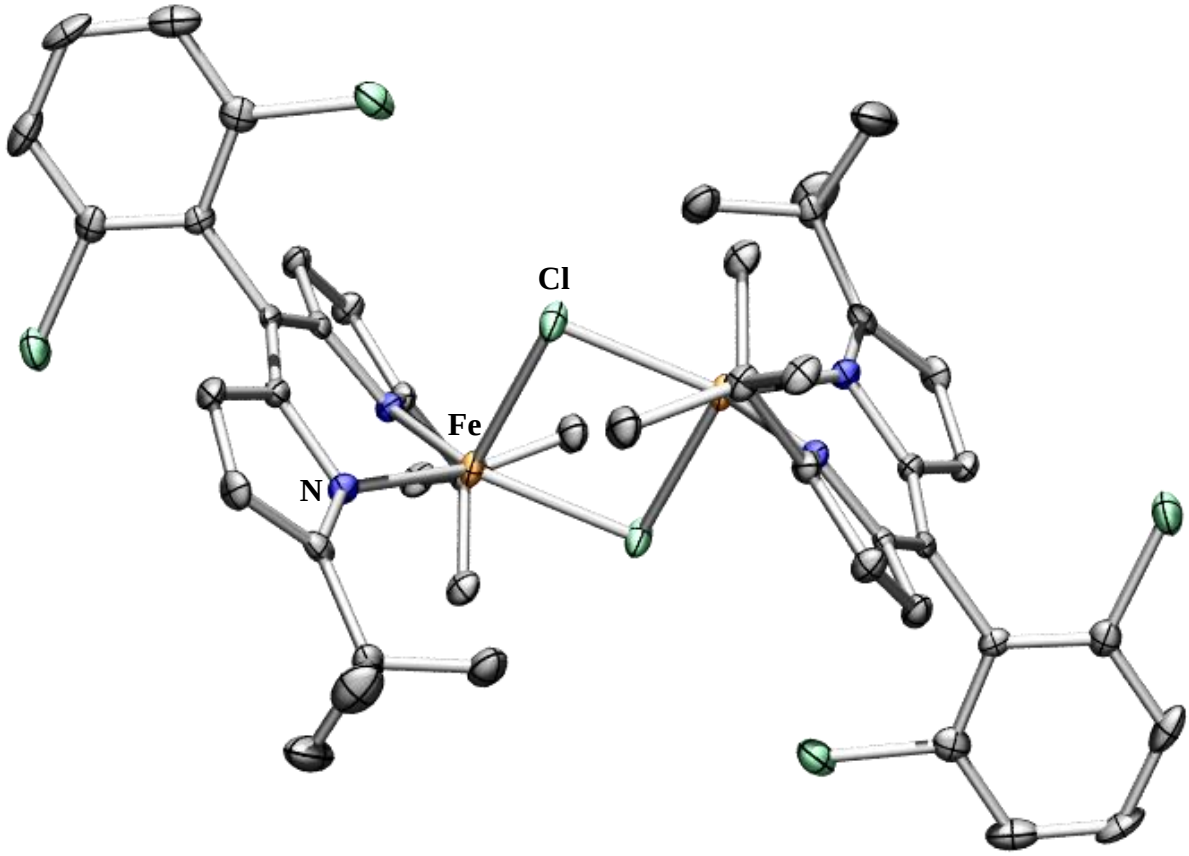

Figure S-33. Solid-state molecular structure for [(^{tBu}L)FeCl]$_2$ (**2**) with thermal ellipsoids at 50% probability level. Hydrogens and benzene solvent in the unit cell were omitted for clarity.

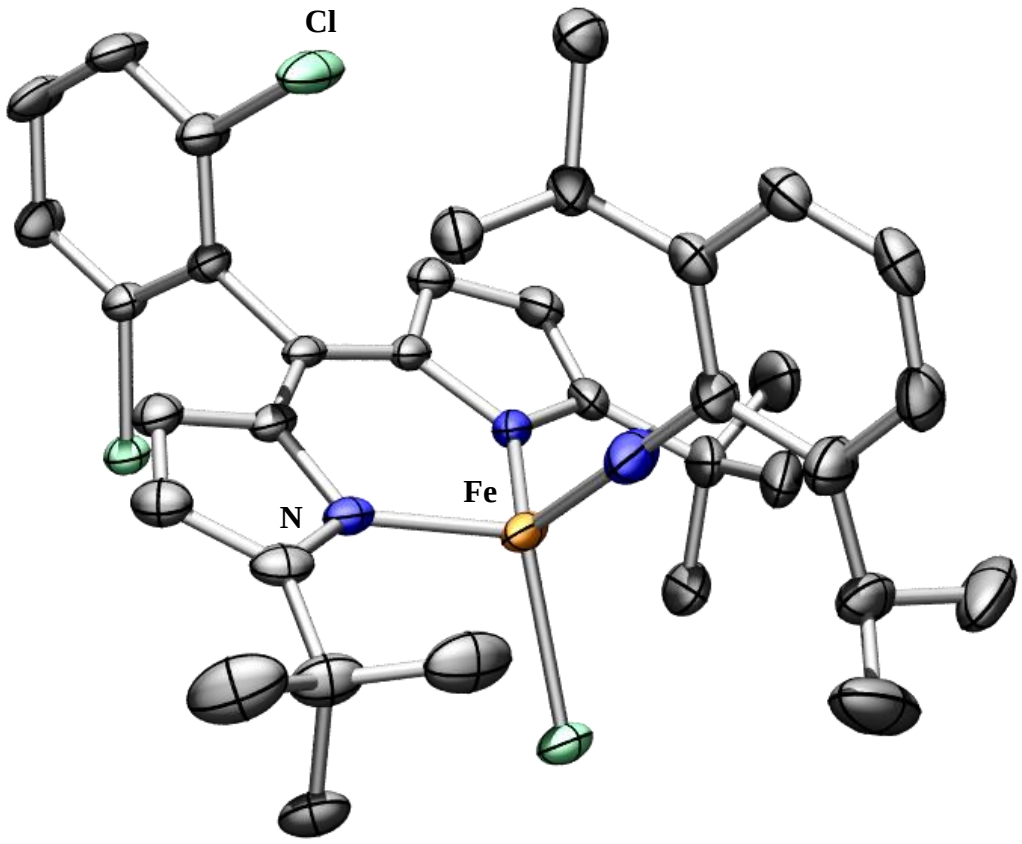

Figure S-34. Solid-state molecular structure for (^{tBu}L)FeCl($^{\bullet}$NC$_6$H$_3$-2,6-^{i}Pr$_2$) (**3**) with thermal ellipsoids at 50% probability level. Hydrogens, disordered isopropyl group and fluorobenzene solvent in the unit cell were omitted for clarity.

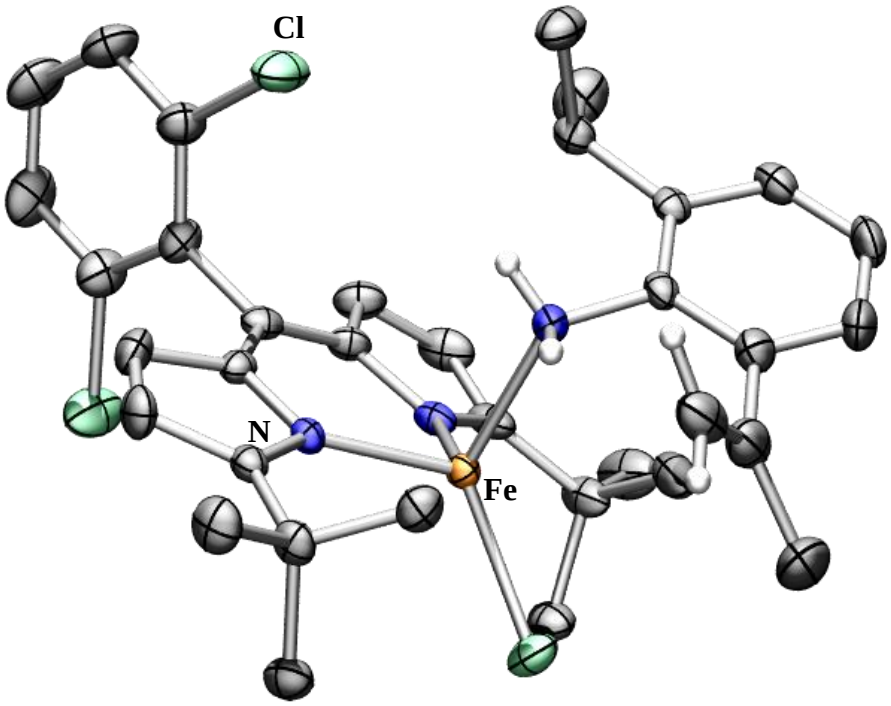

Figure S-35. Solid-state molecular structure for (^{tBu}L)FeCl($H_2NC_6H_3$-2-^{i}Pr-6-C(CH_2)(CH_3)) (**4**) with thermal ellipsoids at 50% probability level. Hydrogens and benzene solvent in the unit cell were omitted for clarity.

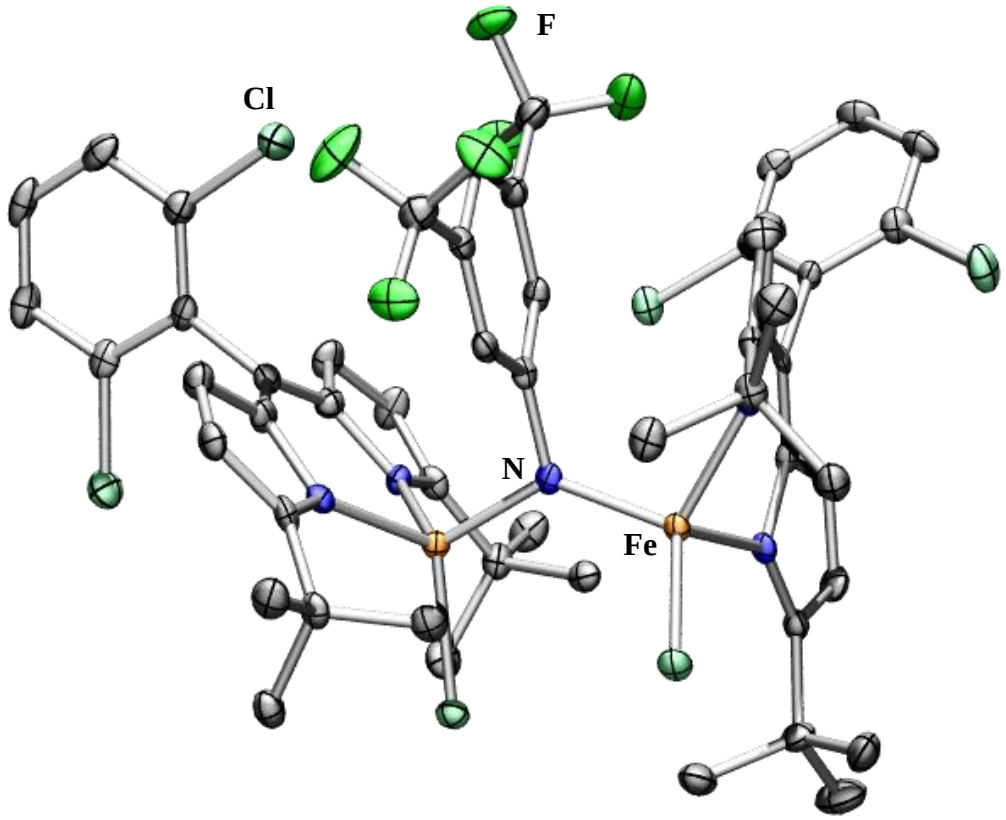

Figure S-36. Solid-state molecular structure for [(^{tBu}L)FeCl]$_2$(μ-NC$_6$H$_3$-3,5-(CF$_3$)$_2$) (**6**) with thermal ellipsoids at 50% probability level. Hydrogens and benzene solvent in the unit cell were omitted for clarity.

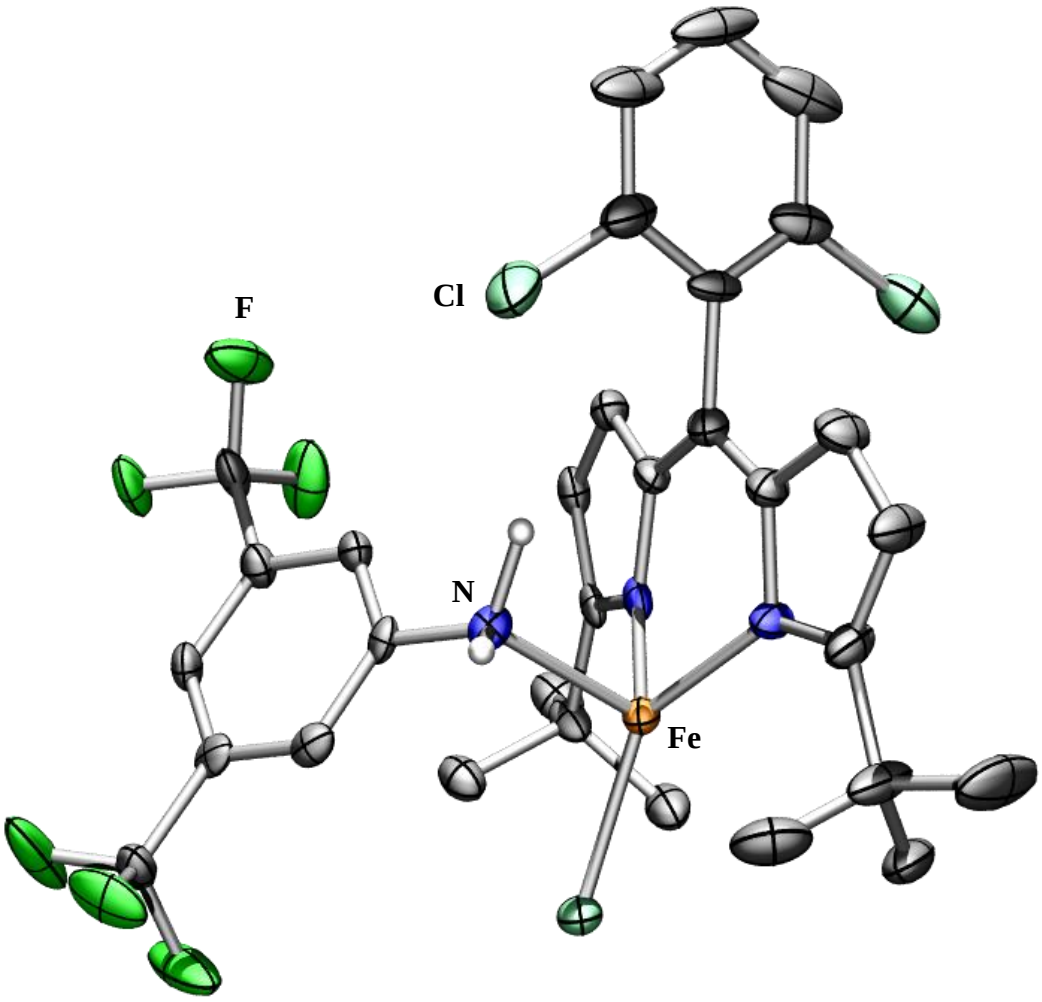

Figure S-37. Solid-state molecular structure for (^{tBu}L)FeCl($H_2NC_6H_3$-3,5-$(CF_3)_2$) (**7**) with thermal ellipsoids at 50% probability level. Hydrogens, disordered trifluoromethyl groups, disordered chloride and benzene solvent in the unit cell were omitted for clarity.

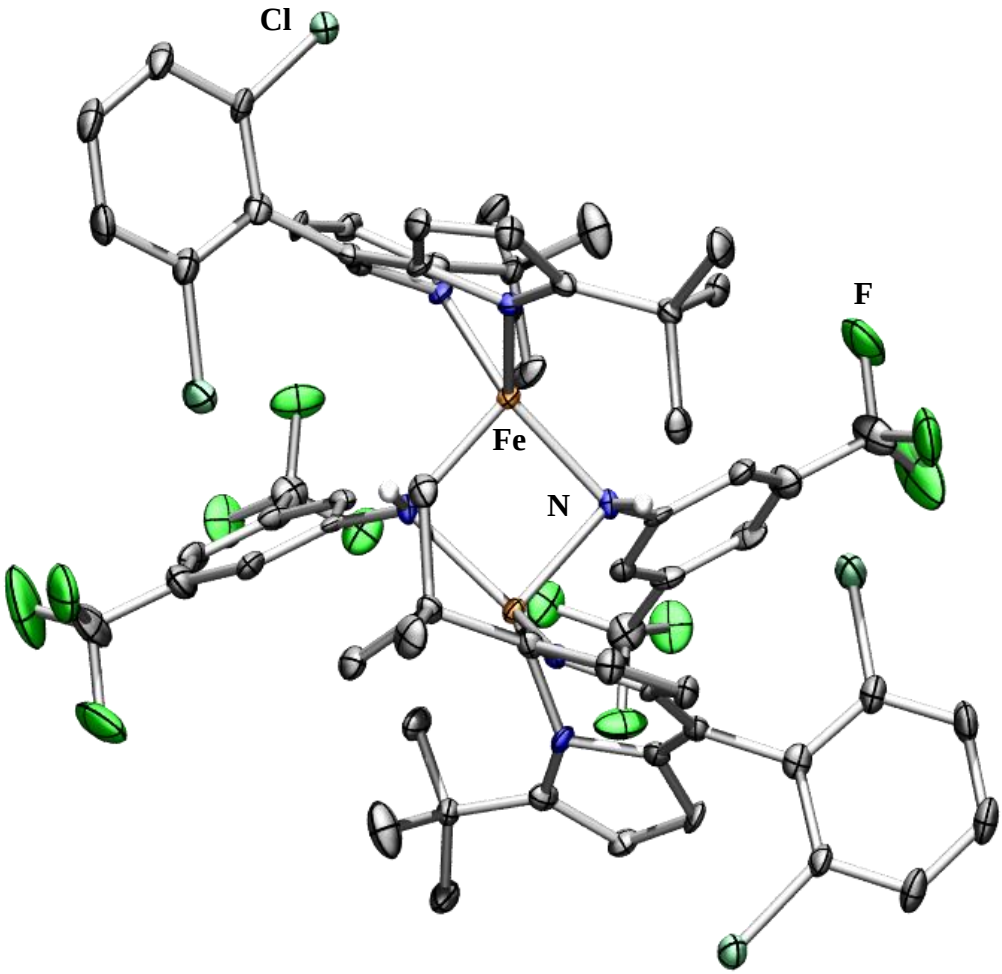

Figure S-38. Solid-state molecular structure for [(^{tBu}L)FeCl(HNC$_6$H$_3$-3,5-(CF$_3$)$_2$)]$_2$ (**8**) with thermal ellipsoids at 50% probability level. Hydrogens and hexanes solvent in the unit cell were omitted for clarity.

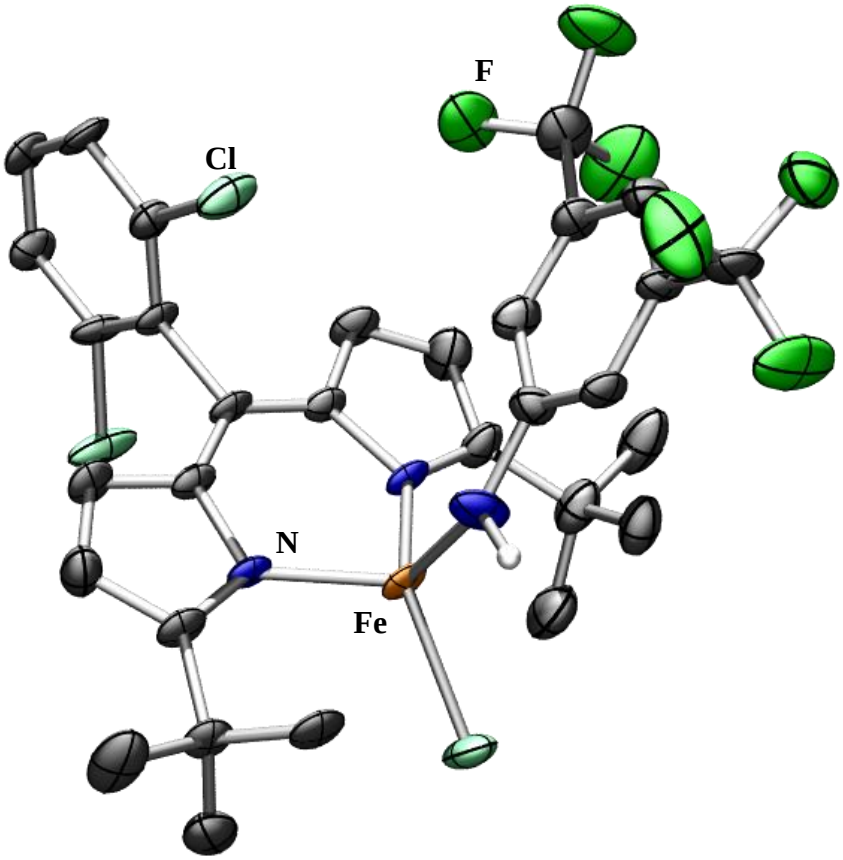

Figure S-39. Solid-state molecular structure for (^{tBu}L)FeCl(HNC$_6$H$_3$-3,5-(CF$_3$)$_2$) (**9**) with thermal ellipsoids at 50% probability level. Hydrogens and benzene solvent in the unit cell were omitted for clarity.

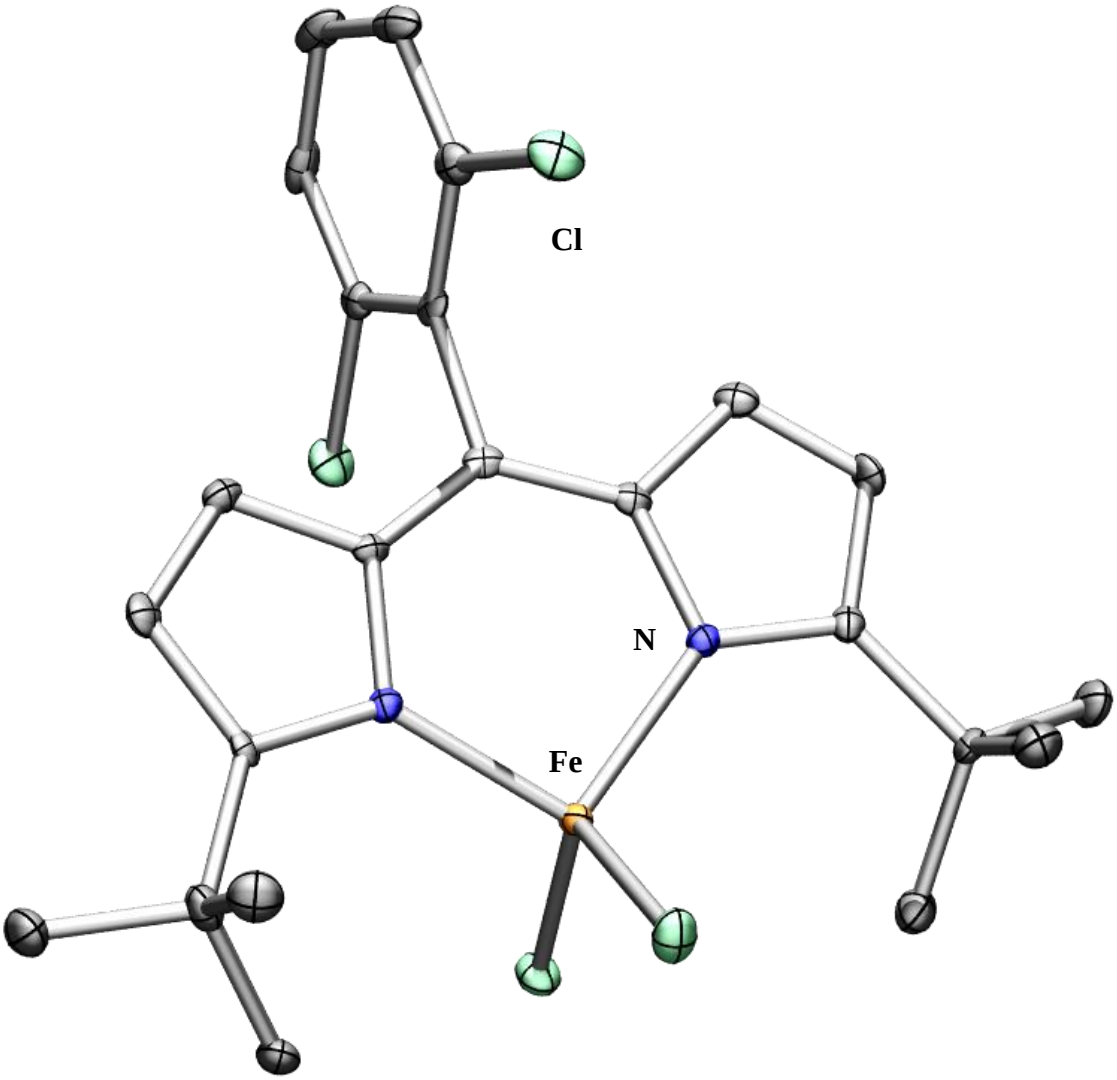

Figure S-40. Solid-state molecular structure for (^{tBu}L)$FeCl_2$ (**10**) with thermal ellipsoids at 50% probability level. Hydrogens were omitted for clarity.

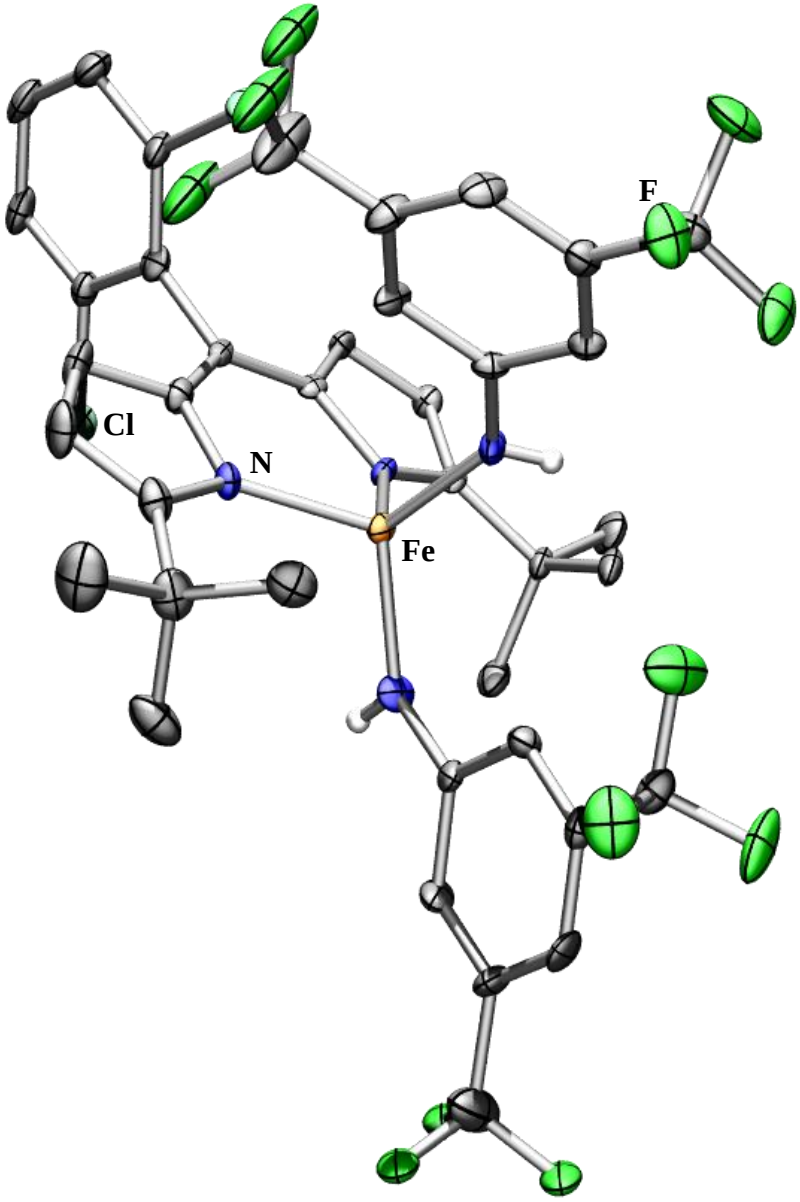

Figure S-41. Solid-state molecular structure for (^{tBu}L)Fe(HNC$_6$H$_3$-3,5-(CF$_3$)$_2$)$_2$ (**11**) with thermal ellipsoids at 50% probability level. Hydrogens and disordered trifluoromethyl groups were omitted for clarity.

Computational Methods. Computations were carried out utilizing the ORCA 2.9[14] program package. The B3LYP[15] functional was used with the def2-TZVP (Fe, N, Cl) and def2-SV(P) (C, H) basis sets[16]. For single point calculations and property calculations the def2-TZVP/J (Fe, N, Cl) and def2-SVP/J (C, H) auxiliary basis sets[17] were employed to utilize the RIJCOSX[18] approximation for accelerating the calculation. For the calculation of Mössbauer parameters the basis set at Fe was expanded to the CP(PPP) basis[19]. All geometries were taken from X-ray structures.

Mössbauer. Mössbauer parameters were obtained from additional single-point calculations, following methods described by F. Neese.[20] Quadrupole splittings (ΔE_Q) were calculated from electric field gradient, Eq. S.2.

$$\Delta E_Q = \tfrac{1}{2} eQV_{zz}\sqrt{1+\tfrac{1}{3}\eta^2} \qquad \text{(S.2)}$$

The nuclear quadruple moment $Q(^{57}\text{Fe})$ was taken to be 0.16 barn.[20] The principal tensor components of the EFG are V_{xx}, V_{yy}, and V_{zz}, from which the asymmetry parameter $\eta = (V_{xx} - V_{yy})/V_{zz}$ can be defined.

Isomer shifts (δ) were calculated from the electron density at the nucleus ρ_0, using a linear equation, Eq. S.3[20], with constants determined by fitting the calculated densities to experimental isomer shifts for a series of iron dipyrromethene complexes synthesized in the lab (with the 5-mesityl-1,9-di(2,4,6-triphenylphenyl)dipyrromethene ligand[21]). The basis sets and functional described above were used for all structures. X-ray coordinates were used, and spin-states were assigned based on experimental Mössbauer data.

$$\delta = a(\rho_0 - C) + b \qquad \text{(S.3)}$$

For this series of compounds the parameters were determined to be C = 11580 au^{-3}, a = –0.355 au^3 mm s^{-1}, and b = 1.418 mm.

---

[14] Neese, F. *ORCA - An ab initio, Density Functional and Semi-empirical Electronic Structure Package*; Version 2.9-00 ed. ed. Universitat Bonn, Bonn, Germany, 2009.

[15] (a) Becke, A. D. *J. Chem. Phys.* **98**, 5648 (1993); (b) Lee, C. T.; Yang, W. T.; Parr, R. G. *Phys Rev. B* **33**, 785 (1988).

[16] (a) Schäfer, A.; Horn, H.; Ahlrichs, R. *J. Chem. Phys*. **1992**, *97***,** 2571; b) Schäafer, A.; Huber, C.; Ahlrichs, R. *J. Chem. Phys.***1994**, *100*, 5829; (c) Weigend, F.; Ahlrichs, R. *Phys. Chem. Chem. Phys.* **2005**, *7*, 3297.

[17] Weigand, F. *Phys. Chem. Chem. Phys.* **2006**, *8*, 1057.

[18] Neese, F.; Wennmohs, F.; Hansen, A.; Becker, U. *Chem. Phys.* **2009**, *356*, 98.

[19] Neese, F. *Inorg. Chim. Acta* **2002**, *337*, 181.

[20] (a) Ye, S.; Tuttle, T.; Bill, E.; Simkhovich, L.; Gross, Z.; Thiel, W.; Neese, F. *Chem. Eur. J.* **2008**, *14*, 10839; (b) Sinnecker, S.; Slep, L. P.; Bill, E.; Neese, F. *Inorg. Chem.* **2005**, *44*, 2245.

[21] King, E. R.; Hennessy, E. T.; Betley, T. A. *J. Am. Chem. Soc.* **2011**, *133*, 4917.

Broken Symmetry Solutions. A broken symmetry solution was used to model the antiferromagnetically coupled Fe^{III} iminyl radical, the dimeric $[(^{tBu}L)FeCl]_2$ and the diiron bridging imido. The broken symmetry notation BS(m,n)[22] refers to a system with (m+n) unpaired electrons, and a net spin of $^{(m-n)}/_2$ (if antiferromagnetically coupled). One fragment will bear m α spin electrons, and the other fragment n β spin electrons.

For the Fe^{III} iminyl radical **3**, BS(5,1) was the appropriate description for a high-spin Fe^{III} ($S = {}^5/_2$) coupled to a imido radical ($S = {}^1/_2$). The corresponding orbital transformation[22], and the resultant corresponding orbital overlap were used as an indicator of a spin-coupled system. One pair of corresponding orbitals had overlap of 0.61, which is significantly less than 1, and suggests a broken symmetry solution. The exchange coupling constant J was determined from the energy difference between the high-spin and broken-symmetry states, using the spin-Hamiltonian in Eq. S.4, and the formula[23] in Eq. S.5.

$$H = -2J\vec{S}_{Fe} \cdot \vec{S}_{NR} \tag{S.4}$$

$$J = -\frac{E_{HS} - E_{BS}}{\langle S^2 \rangle_{HS} - \langle S^2 \rangle_{BS}} \tag{S.5}$$

Based on the energy difference of $E_{HS} - E_{BS}$ = 3528.839 cm^{-1}, the antiferromagnetic coupling constant is estimated to be J = –655 cm^{-1}.

For the $[(^{tBu}L)FeCl]_2$ **2**, BS(4,4) was the appropriate description for two weekly coupled high-spin Fe^{II} (S = 2) centers. Based on the energy difference of $E_{HS} - E_{BS}$ = 110.721 cm^{-1}, the antiferromagnetic coupling constant is estimated to be J = –6.92 cm^{-1}.

For the bridging imido **6**, BS(5,5) was the appropriate description for two weekly coupled high-spin Fe^{III} ($S = {}^5/_2$) centers. The corresponding orbital transformation[22], and the resultant corresponding orbital overlap were used as an indicator of a spin-coupled system. Two pairs of corresponding orbitals had overlap of 0.35 and 0.32, which is significantly less than 1, and suggests a broken symmetry solution. Based on the energy difference of $E_{HS} - E_{BS}$ = 3039.011 cm^{-1}, the antiferromagnetic coupling constant is estimated to be J = –120 cm^{-1}.

[22] Kirchner, B.; Wenmohs, F.; Ye, S.; Neese, F. *Curr. Opin. Chem. Biol.* **2007**, *11*, 134.
[23] (a) Yamaguchi, K.; Takahara, Y.; Feuono, T. in *Applied Quantum Chemistry* (Eds.: V. H. Smith), Reidel, Dordrecht, p. 586 (1986); (b) Soda, T.; Kitigawa, Y.; Onishi, T.; Takano, Y.; Shigeta, Y.; Nagao, H.; Yoshioka, Y.; Yamaguchi, K. *Chem. Phys. Lett.* **2000**, *319*, 223.